Lamprey Lecticans Link New Vertebrate Genes to the Origin and Elaboration of Vertebrate Tissues

Zachary D. Root[1], David Jandzik[1,2], Cara Allen[1], Margaux Brewer[1], Marek Romášek[1], Tyler Square[1,3], Daniel M. Medeiros[1]*

1 Department of Ecology and Evolutionary Biology, University of Colorado, Boulder, CO 80309, USA

2 Department of Zoology, Comenius University in Bratislava, Bratislava, 84215, Slovakia

3 Department of Molecular and Cellular Biology, University of California, Berkeley, CA 94720, USA

* Author for correspondence

ABSTRACT

The evolution of vertebrates from an invertebrate chordate ancestor involved the evolution of new organs, tissues, and cell types. It was also marked by the origin and duplication of new gene families. If, and how, these morphological and genetic innovations are related is an unresolved question in vertebrate evolution. Hyaluronan is an extracellular matrix (ECM) polysaccharide important for water homeostasis and tissue structure. Vertebrates possess a novel family of hyaluronan binding proteins called Lecticans, and studies in jawed vertebrates (gnathostomes) have shown they function in many of the cells and tissues that are unique to vertebrates. This raises the possibility that the origin and/or expansion of this gene family helped drive the evolution of these vertebrate novelties. In order to better understand the evolution of the *lectican* gene family, and its role in the evolution of vertebrate morphological

novelties, we investigated the phylogeny, genomic arrangement, and expression patterns of all *lecticans* in the sea lamprey (*Petromyzon marinus*), a jawless vertebrate. Though both *P. marinus* and gnathostomes have four *lecticans*, our phylogenetic and syntenic analyses suggest lamprey *lecticans* are the result of one or more cyclostome-specific duplications. Despite the independent expansion of the lamprey and gnathostome *lectican* families, we find highly conserved expression of *lecticans* in vertebrate-specific and mesenchyme-derived tissues. We also find that, unlike gnathostomes, lamprey expresses its *lectican* paralogs in distinct subpopulations of head skeleton precursors, potentially reflecting an ancestral diversity of skeletal tissue types. Together, these observations suggest that the ancestral pre-duplication *lectican* had a complex expression pattern, functioned to support mesenchymal histology, and likely played a role in the evolution of vertebrate-specific cell and tissue types.

INTRODUCTION

The emergence of vertebrates involved the elaboration of the ancestral chordate body plan with an array of new cell types, tissues, and organs. Among these are the expanded central and peripheral nervous systems, and the complex skeletomuscular systems of the head and trunk, which includes an array of new structural and connective tissues [1, 2]. Interestingly, large portions of these novelties are derived from the same embryonic source, neural crest cells, which also give rise to parts of the heart, teeth, endocrine system, and vascular smooth muscle [1-3]. The evolution of these morphological and developmental novelties coincided with major genome-wide changes including the origin of several new gene families, at least one whole genome duplication, and the evolution of new gene regulatory networks [4-15]. The timing of these genomic events has led to speculation that they facilitated the origin and morphological diversification of vertebrates by altering early development.

While alterations in embryogenesis can lead to major changes in the body plan, the evolution of truly novel tissues and cell types also requires the evolution of new cellular

functions and histological properties. Extracellular matrix (ECM) proteins not only provide support and structure to cells and tissues, but also mediate signal transduction and mechanotransduction [16]. A key component of the ECM of many vertebrate tissues is a vertebrate-specific family of proteoglycans called Lecticans. Structurally, Lecticans are complex, consisting of hyaluronan-binding X-link domains, c-type lectin domains, a chondroitin/keratan sulfate binding domain, and an immunoglobulin domain. Because of this modular structure, Lecticans are able to interface with many different types of molecules and perform a range of functions in the ECM of diverse cells and tissues [17].

Genomically, all gnathostome *lectican* paralogs are closely linked to a *hapln* gene, which also encodes an X-link domain containing protein [18]. The proximity of *lecticans* and *haplns*, together with their high sequence similarity, indicate they evolved via tandem duplication of an ancestral X-link protein-encoding gene, with subsequent exon shuffling resulting in the hybrid structure of Lecticans [19]. After assembly of the primordial *lectican* gene, two genome-wide duplications are thought to have generated the four paralogs seen in modern jawed vertebrates: *aggrecan* (*acan*), *brevican* (*bcan*), *neurocan* (*ncan*), and *versican* (*vcan*). Since these duplications, the structures of the four gnathostome Lecticans have diverged, with *acan* acquiring an additional, X-link domain, *bcan* and *ncan* losing an interglobular fold sequence adjacent to the immunoglobulin domain, and all Lecticans evolving chondroitin/keratan sulfate binding domains of different sizes [17].

Subfunctionalization, specialization, and/or neofunctionalization of gnathostome *lectican* paralogs resulted in each possessing distinct expression patterns and functions, in neural, skeletal, cardiac, and connective tissues [20, 21]. *acan* is known primarily for its role in the cartilage ECM [22, 23] [among others], but it is also involved in neural crest cell migration and synaptic complexes in the brain [24-28]. *acan* expression has also been found in the developing notochord as well as the epicardium and mesenchyme of the heart [29, 30]. *vcan* is the most widely expressed *lectican* and is transcribed in mesoderm-derived tissues and organs including

the kidneys, heart, muscles, and skeleton [29-34], and various neurectodermal derivatives like the otic vesicle, lens primordium [32], oligodendrocytes, Schwann Cells, the perineuronal net, ectodermal placodes, and migrating neural crest cells [20, 28, 35-38]. *bcan* and *ncan* are primarily expressed in the nervous system [20, 26, 39-49], though notochord and heart expression has also been reported [46, 50-52]. Of the four *lecticans*, mutation of *acan* leads to the most significant defects, including severe chondrodysplasia [23], while *vcan* loss-of-function causes abnormal eye and heart development [53-55]. The functions of *bcan* and *ncan* are less clear, however, as mice deficient in these genes show only minor defects in neuronal potentiation [56, 57].

It has been proposed that the evolution of novel interactions between Lecticans, hyaluronan, and other glycoproteins played an important role in the evolution of vertebrate tissues [19]. However, our understanding of *lectican* expression, function, and evolution is based entirely on the information from model gnathostomes. It is thus unclear when in the vertebrate lineage *lecticans* originated, were duplicated, and acquired their diverse functions. The only two living jawless vertebrates, the lampreys and hagfish (the cyclostomes) have been indispensable for understanding vertebrate evolution [58-62]. These modern agnathans diverged from the lineage leading to gnathostomes around 500 million years ago [63, 64]. Due to accessibility, lampreys are the best studied of the two, and historical and modern molecular comparisons have shown that lamprey and gnathostomes share many core aspects of their development[58, 65-69].

In this study, we used genomic and transcriptomic data from the sea lamprey, *Petromyzon marinus* to gain insight into the evolutionary history of *lectican* genes. These data support independent expansion of the *lectican* family in the lamprey and gnathostome lineages. We also characterized the expression patterns of *lecticans* in sea lamprey embryos and larvae, and show that *lectican* expression in neural, cardiac, and skeletal tissue is highly conserved across living vertebrates. In contrast, we find that expression of *lectican* paralogs in the head

104 skeleton is markedly different between lamprey and gnathostomes. We posit that the ancestral
105 pre-duplication *lectican* had a complex expression pattern which was independently partitioned
106 between paralogs in the lamprey and gnathostome lineages. We further speculate that the
107 primordial Lectican protein functioned to facilitate mesenchymal histology and behavior in the
108 first vertebrates.
109
110 **RESULTS**
111 **The sea lamprey has four *lectican* genes encoding proteins with similar domain**
112 **structures**
113 We searched the *P. marinus* germline genome [70] and identified four different genomic
114 scaffolds containing exons with sequence similarity to gnathostome Lecticans. We also
115 searched all publicly available lamprey transcriptome data, as well as our own database of
116 transcriptome sequences (see Methods) for gnathostome *lectican*-like sequences, and
117 assembled these into 4 mRNAs corresponding to proteins of 1871aa, 1757aa, 1825aa, and
118 1343aa respectively (see Tab. S3 for accession numbers). All identified *lectican* exons aligned
119 to parts of the reconstructed mRNAs, indicating there are only four sea lamprey *lectican* genes.
120 We named these genes *lecticanA* (*lecA*), *lecticanB* (*lecB*), *lecticanC* (*lecC*), and *lecticanD*
121 (*lecD*). We then searched for conserved domains in lamprey *lectican* conceptual translation
122 products using NCBI's Conserved Domain search tool, and by alignment with gnathostome
123 Lecticans. We found that although all lamprey Lectican protein sequences had largely
124 archetypical domain structures, at least one domain appeared to be missing in each [Fig. 1A].
125 LECA and LECC did not possess an identifiable complement control protein domain, while
126 LECB did not have an immunoglobulin-like domain, and LECD did not have EGF-like domains.
127 We also found that no lamprey Lectican possessed the extra X-link domain seen in ACAN [Fig.
128 1A].
129

Phylogenetic analyses do not support one-to-one orthology of lamprey and gnathostome *lecticans*

To deduce relationships between lamprey and gnathostome *lecticans*, we used *lectican* protein sequences to perform maximum likelihood phylogenetic analyses, with different taxa, substitution models, and individual parameters for tests [71-74] [Fig. S1,S2,S3,S4]. Among gnathostome *lecticans*, we recovered all four known paralog groups and found good support for *acan+bcan* and *vcan+ncan* subfamilies. In contrast, we found that none of the lamprey Lecticans consistently group within any of the four gnathostome Lectican paralogy groups, nor the *acan+bcan* and *vcan+ncan* subfamilies regardless of the parameters used to build the phylogenies [Fig. 1B, Fig. S5]. Lamprey *lecticans* and *hapln*s likely originated from a tandem duplication event early in the vertebrate lineage. We reasoned that building a phylogenetic tree using HAPLNs and the HAPLN-aligning portion of Lectican protein sequences might help resolve the relationships between lamprey and gnathostome Lecticans [Fig S4]. As with the full-length Lectican phylogeny, none of the lamprey Lecticans grouped with any gnathostome paralogy group with high confidence.

Analyses of syntenic genes also fails to conclusively support one-to-one orthology between lamprey and gnathostome *lectican* paralogs

All gnathostome *lectican* paralogs are adjacent to a corresponding HAPLN paralog [18]. We thus searched for HAPLN-like reading frames in the lamprey genome [70], and used these to create a phylogeny of chordate HAPLN-related genes in hopes of resolving the relationships between vertebrate *lectican/HAPLN* loci. We identified one lamprey *HAPLN* gene linked to *lecticanD*. However, as with lamprey Lecticans, lamprey HAPLN fails to group convincingly with any single gnathostome paralogy group [Fig. S6]. We also found that gnathostome HAPLN1s and HAPLN4s form a weakly supported clade, consistent with the relationships of their adjacent *lecticans, vcan* and *ncan*. We expanded our search to include other possible conserved

syntelogs. We found that all gnathostome and lamprey *lecticans* are linked to paralogs of the myocyte enhancer factor *mef2* gene family. We thus created a phylogenetic tree of MEF2 amino acid sequences to see if it could provide insights into the evolution of the vertebrate *lectican* locus. As with HAPLN genes, none of the lamprey MEF2 sequences clustered convincingly with any gnathostome MEF2 paralogy group using any parameters [Fig. S7].

As a final test of orthology between lamprey and gnathsotome *lecticans*, we compared the gene complement around the gnathostome and lamprey *lectican* loci. For each lamprey *lectican*, we asked if any of the surrounding 40 genes (when available) had homologs that were syntenic with any chick, spotted gar, or elephant shark *lecticans* [Fig. 2A, Fig. S8]. We found that *lecA* had the most conserved syntelogs, with 21/40 of adjacent genes having gnathostome homologs closely linked to one or more *lecticans* (i.e. syntelogs). Of those, 15 were exclusively linked to an *acan* or a *bcan*, while only 4 were exclusively linked to a *vcan* or *ncan*. Around the *lecB*, *lecC*, and *lecD* loci, 30-40% of genes had unambiguous gnathostome syntelogs, with similar proportions linked to the *acan*+*bcan* versus *vcan*+*ncan* subfamilies [Fig. S8]. Thus, comparisons of syntelogs provide some support for placing *lecA* in the *acan*+*bcan* subfamily [Fig 2B].

Expression of *lecticans* in sea lamprey embryos and larvae

We first detected *lecA* expression at Tahara [75] stage 21 (st. T21) in the presumptive neural tube and newly formed somites [Fig. 3A]. At st. T23, we continued to see lecA expression in these regions, and sectioning revealed transcripts in the notochord, neural tube floor plate, and sclerotome [Fig. 3C, 3C']. *lecA* transcripts were also detected in the developing myocardium at this stage. By T24 and T25, *lecA* expression expanded into the posterior lateral line ganglia, zona limitans intrathalamica, and the telencephalon [Fig. 3D, D', D'']. At stage T26, we observed new expression in the posterior heart tube [Fig 3E]. At this stage, *lecA* transcripts were also found in skeletogenic mesenchyme in the pharynx and oral region, and in the fin fold

mesenchyme [Fig 3E', E''']. We also noted that expression of *lecA* in the maturing pharyngeal arches was highly dynamic, with activation and downregulation occurring in an anterior to posterior wave. By st. T27, this pharyngeal mesenchyme cell expression was limited to the oral hood, outer velum, and lips [Fig 3F]. At stage T28, *lecA* was almost entirely restricted to the mucocartilage of the oral hood, velum, and fin fold [Fig 3G, G', 3I, I'].

Expression of *lecB* was first observed at stage T23 in the oral ectoderm [Fig 4A]. This expression remained similar until mid pharyngula at (T25) when *lecB* expression expanded into the lateral neural tube [Fig 4B, B']. By middle-late pharyngula at stage T25 and T26, *lecB* was observed in the pronephros [Fig 4C, 4D]. We also identified *lecB* expression in the nasohypophyseal and ophthalmic, lens, and maxillomandibular placodes as well as the basolateral hypothalamus [Fig 4D']. As skeletogenesis began at stages T26.5 and T27, we identified *lecB* transcripts in the mucocartilage of the outer velum, lips, and ventrolateral pharyngeal bars [Fig 4E, E']. At these stages, we were able to confirm *lecB* expression in the pharyngeal endoderm through sectioning. However, by stage T27, this expression began to fade in an anterior-posterior manner. We no longer detected *lecB* in the developing brain or neural placodes likewise at these stages. By stage T28, *lecB* was primarily found in the medioventral cartilage bar and the developing oral papillae [Fig 4F, F'].

Strikingly, *lecC* expression was only observed in forming cell-rich hyaline cartilage bars in the head skeleton. This expression closely tracks alcian blue reactivity, as previously described [76]. We first detected *lecC* transcripts at stage T26.5 in neural crest in the intermediate domain of the third through sixth pharyngeal arches [Fig 5A]. This expression expanded to the seventh and eighth arch cartilage bars, and by stage T28, *lecC* expression was seen in all hyaline cartilage bars in the posterior pharynx, as well as the trabeculae [Fig 5C, C'].

We identified *lecD* expression at stage T21 in the developing somites [Fig 6A]. By early pharyngula in stage T23, *lecD* was additionally found in the splanchnic mesoderm [Fig 6B, B']. At this stage, our sectioning confirmed expression in the somites to be localized in the

sclerotome [Fig 6B']. Expression in the somite abated by stages T24 and T25, starting in the anterior somites and moving posterior [Fig 4C]. At stage 26, we detected *lecD* in the posterior endocardium and heart tube as well as the ventral aorta [Fig 4D, 4D']. By late pharyngula at stages T26.5 through T27, *lecD* was expressed in the entirety of the aortic arches in the pharynx as well as the mucocartilage of the lower lip and ventral pharynx surrounding the endostyle [Fig 4E, F, F', F'']. Expression in the aortic arches and ventral mucocartilage dissipated by stage T28, but we continued to see expression in the heart tube, lower lip mucocartilage, and ventral aorta [Fig 4G, G' G''].

DISCUSSION

The evolution of vertebrate developmental and morphological novelties has been linked to a variety of genetic and genomic events, including the evolution of new gene regulatory interactions between ancient developmental regulators, the origin of new gene families, and genome-wide duplication events [5, 7, 13, 15, 77]. To better understand the role of new gene families and gene duplications in vertebrate morphological evolution, we investigated the phylogeny and expression of *lectican* genes in the sea lamprey. To our knowledge, this work constitutes the first comprehensive expression analysis of all *lecticans* in a single vertebrate, and the first description of these genes in a jawless vertebrate.

Evolutionary history of the *lectican* family

Gnathostome *lecticans* and the related *haplns* are thought to have arisen via tandem duplication of a *hapln*-like gene sometime in the vertebrate lineage, with *lecticans* later gaining their complex domain structure by exon shuffling. Consistent with this scenario, we found one lamprey *hapln* closely linked to the *lecD* locus [Fig. 2A]. The timing of the duplication events that created the gnathostome and lamprey *lectican* families is less clear. Like previous reports, our phylogenetic analyses place all gnathostome *lecticans* into four paralogy groups, with

acan+bcan and *vcan+ncan* forming two subfamilies. This topology is typical of gnathostome gene families and strongly suggests the four gnathostome *lecticans* were generated during the two vertebrate genome-scale duplication events (1R and 2R) [4, 78-80]. In contrast, the relationships among lamprey *lecticans*, and between lamprey and gnathostome *lecticans*, are inconclusive. Regardless of tree building parameters, lamprey *lectican*s fail to consistently group with gnathostome paralogy groups, often clustering weakly with each other [Fig. 1B]. Phylogenetic analyses of the neighboring genes *hapln* and *mef2,* and comparisons of syntenic genes yielded similarly inconclusive and weakly-supported phylogenies. There are several scenarios that could account for lack of clear one-to-one orthology between lamprey and gnathostome *lectican*s. One explanation is that the lamprey and gnathostome *lectican*s are the result of independent duplications of a single ancestral *lectican* in each lineage. At the other extreme, lamprey *lectican*s could be fast-evolving cryptic orthologs of gnathostome *lectican*s generated by the two vertebrate genome-wide (2R) duplication events. Various scenarios involving shared duplication, gene loss, and independent duplication are also possible. A prerequisite for cryptic one-to-one orthology is that lamprey diverged from gnathostomes after the 2R genome duplications. However, recent comprehensive comparisons of chordate genome structure refute this, showing lamprey most likely diverged from gnathostomes before the second, “2R”, genome duplication [4, 81]. If this is the case, the common ancestor of lamprey and gnathostomes likely had two *lectican*s, an ancestral *acan+bcan* and an ancestral *vcan+ncan*. Consistent with this, we find that the genomic region surrounding *lecA* is *acan+bcan*-like but shows no particular similarity to either the *acan* or *bcan* regions (Tab. S1). In contrast, we find that none of the other lamprey *lectican* genomic regions are *ncan* and/or *vcan*-like. Taken together, our data support the presence of two *lectican*s in the last common ancestor of lamprey and gnathostomes, with one or both being duplicated in the cyclostome lineage to yield the four lamprey *lectican*s [Fig. 2B]. Of these, *lecA* is likely derived from the *acan+bcan*-related 1R duplicate, while the orthology of *lecB*, *lecC*, and *lecD* and gnathostome

lecticans is unresolved [Fig. 2B]. Although *lecB*, *lecC* and/or *lecD* could be cryptic *vcan+ncan* family members, it is also possible the *vcan+ncan* subfamily was lost in the lamprey lineage, and all lamprey *lecticans* are *acan+bcan* co-orthologs [Fig. 2B].

Lectican expression in the nervous system is ancestral within vertebrates

Regardless of their phylogenetic relationships, we found that almost every gnathostome *lectican* expression domain was conserved in lamprey, with only a few minor differences. To what degree these differences reflect divergence in *lectican* regulation between lamprey and gnathostomes, or the incomplete documentation of *lectican* expression in gnathostomes, is unclear. In the central nervous system, *lecA* and frog *vcan* both display expression in the neural tube floor plate [Fig 3C'] [30]. Lamprey *lecB* expression is also observed in the lateral neural tube [Fig 4B'], though there are no reports of gnathostome *lectican* transcription in this region. *lecA* and *lecB* are expressed in the developing brain like *bcan* and *ncan* [Fig 3D', D'', Fig 4D'], though not as broadly. Like *ncan*, *bcan*, and *vcan, lecA* and *lecB* are expressed in the cranial placodes and sensory ganglia [Fig 3D', D'', Fig 4D'], though in different neural populations [38, 46, 47]. Although *lectican* expression in the forming nervous system appears to conserved among living vertebrates, the role of *lecticans* in neural development is unclear, as *bcan* and *ncan*-deficient mice show only minor differences in neuron function [56, 57]. Regardless of their precise functions, our data suggest that the LCA of cyclostomes and gnathostomes expressed *lecticans* in both the peripheral and central nervous systems.

Lectican expression in mesoderm-derived tissues is conserved across vertebrates

As in the forming nervous system *lectican* expression in mesodermal derivatives is largely conserved between lamprey and gnathostomes. In the gnathostome heart, *aggrecan* marks migratory cardiac mesoderm [29], while *ncan* marks the forming myocardium and splanchnic mesoderm, and *vcan* marks the endocardium and the heart tube [29, 46, 51, 82]. In

lamprey, *lecA* is expressed in the myocardium [Fig 3E''] while *lecD* marks the posterior endocardium and heart tube as well as the ventral aorta [Fig 6D']. As in neural tissue, the precise role of *lectican*s in the gnathostome heart is unclear, though mouse *vcan* mutants have major defects in the developing heart tube and endocardial cushion [53-55].

Aside from cardiac mesoderm, we also noted expression of one or more lamprey *lectican*s in the notochord [Fig 3C'], pronephros [Fig 4C], fin mesenchyme [Fig 3I], and sclerotome [Fig 3C', 4B', 6B']. All of these mesodermal tissues express one or more *lectican*s in gnathostomes in temporal and spatial patterns virtually identical to their lamprey counterparts. The only notable difference in mesodermal *lectican* expression we observed was an absence of lamprey *lectican*s in somatic lateral plate mesoderm (LPM), which gives rise to *acan* and vcan-expressing skeletal tissue in gnathostome paired fins and limbs.

Combinatorial *lectican* expression suggests lamprey possesses a diverse array of neural crest-derived skeletal tissues

We find that expression of multiple *lectican*s in forming and differentiated skeletal tissue is a conserved feature of vertebrate development. However, we also noted that gnathostomes typically transcribe only two *lectican*s in skeletogenic neural crest cells, *acan* and *vcan*, whereas lamprey expresses all four. Furthermore, lamprey *lecticans* are expressed in spatiotemporally distinct patterns throughout development, creating a combinatorial code of *lectican* expression in different parts of the nascent lamprey head skeleton. The histological heterogeneity of the lamprey head skeleton, which includes a mesenchymal chondroid tissue called mucocartilage, has been noted before [83-89]. Anatomical work on adult hagfishes has also revealed diverse histology in the head skeleton [90-93], suggesting that the LCA of cyclostomes likely had multiple chondroid tissue types. It is possible the combinatorial co-expression of *lectican*s in the lamprey head skeleton elements reflects histological differences between different subtypes of mucocartilage. If this is the case, it would suggest that either 1) the LCA of cyclostomes and

gnathostomes had a diversity of neural crest-derived chondroid tissues and the gnathostome lineage has retained only a few; or 2) the LCA of cyclostomes and gnathostomes had only a few neural crest-derived cartilage subtypes and the diversity seen in the sea lamprey head skeleton is a derived feature of lampreys, or cyclostomes. It has been previously shown that the pharyngeal skeleton of cyclostomes is patterned using the same basic mechanisms as seen in gnathostomes [9, 66, 88, 94-97] . In gnathostomes, this patterning acts a scaffold for proper deployment of the morphogenetic programs that control skeletal element shape and the tissue differentiation. In lamprey, which has a largely symmetrical oropharygneal skeleton, this patterning may function mainly to control the activation of distinct differentiation programs in different parts of the head skeleton as previously proposed [66, 95, 96].

Different patterns of specialization and subfunctionalization after *lectican* duplication in lamprey and gnathostomes

Gene duplication is thought to facilitate evolutionary novelty by creating additional copies of genes that can then diverge to gain new expression domains and functions (neofunctionalization). More commonly, however, duplication leads to partitioning of ancestral expression domains (subfunctionalization) as described by the duplication-degeneration-complementation model [98]. Recent functional genomic comparisons have also highlighted the importance of specialization after duplication in the vertebrate lineage. During specialization, one paralog loses most aspects of its ancestral expression pattern and becomes specialized for a particular domain, while other paralogs maintain the complete ancestral pattern [12]. Our data suggest the ancestral *lectican* had a complex expression pattern, and was independently duplicated in the lamprey and gnathostomes, with little apparent neofunctionalization in either lineage [Fig. 7]. We also find that the relative roles of specialization and subfunctionalization differ between the gnathostome and lamprey *lectican* families. Striking specialization is apparent in the lamprey *lectican* family, where *lecA* is transcribed in virtually all major *lectican* expression

domains, while *lecC* has highly restricted expression in cell-rich hyaline cartilage [Fig. 7]. Similarly, *lecD* transcripts are only seen in the sclerotome, heart, and a subpopulation of skeletogenic NCCs. In contrast, no gnathostome *lectican* is so strictly specialized, and all paralogs are expressed in partially overlapping subsets of the ancestral expression pattern that could be described as "overlapping subfunctionalization" [22, 23, 25, 29, 33, 34, 39, 44, 45, 50] [Fig. 7]. Whether the different modes of expression pattern evolution have any significant consequences for Lectican protein function is unclear. Specialization of ohnologs is usually associated with rapid divergence in protein coding sequence [12]. Contrary to this prediction, lamprey *lecC*, the most specialized lamprey *lectican*, and *lecA*, the most broadly expressed lamprey *lectican* have similar, archetypical *lectican* structures. Meanwhile, all gnathostome *lecticans* vary significantly in length, and have lost and gained different functional domains. Nevertheless, it is provocative that both lamprey and gnathostomes typically express multiple *lecticans* in each expression domain. This suggests Lectican proteins are not entirely redundant, and supports the idea that combinations of functionally distinct Lectican proteins may confer subtle histological differences in related tissues.

The primordial *lectican* likely contributed to the evolution of vertebrate traits and functioned to support mesenchymal histology

Vertebrate evolution involved the acquisition of new organs, tissues, and cell types, as well as the elaboration of many pre-existing cell and tissue types. The *lectican* family is also a vertebrate novelty that arose at around the same time as these histological and morphological innovations. To what degree the evolution of new gene families drove the evolution of vertebrate traits is an open question. We used our expression data to ask if *lectican*-expressing cells and tissues were usually vertebrate novelties, or had clear homologs in invertebrate chordates [Tab. 1]. If a recognized homolog was present, we next asked if the histology of the vertebrate cell/tissue differed fundamentally from its invertebrate counterpart.

These comparisons reveal that *lectican* transcription is largely restricted to cells and tissues that are either *bona fide* vertebrate novelties, or have unique histology in vertebrates.

If *lecticans* are indeed expressed mainly in vertebrate histological innovations, what specifically did the first *lectican* contribute to the vertebrate phenotype? Perhaps the best studied Lectican is Aggrecan, which is a major component of the hyaline cartilage ECM, and confers many of its defining histological and structural properties. It was previously thought that hyaline cartilage was unique to vertebrates, though a clear homolog with virtually all of its defining features has recently been described in the invertebrate chordate amphioxus[99]. Thus, the origin of the first *lectican* was likely not prerequisite for the evolution of vertebrate-type cellular cartilage. Nevertheless, it is possible that *lecticans* contributed to the evolution of a more rigid type of cell rich hyaline cartilage, or the evolution of ECM-rich hyaline cartilage [Tab. 1].

Aside from hyaline cartilage, *lecticans* are expressed in a variety of other tissues during development. This suggests the evolution of the first *lectican* conferred a more general property upon vertebrate cells and tissues. Provocatively, a common theme among *lectican*-expressing cell types is that they differentiate from migratory and/or mesenchymal precursors [Tab. 1]. Furthermore, gnathostome *lecticans* have been shown to regulate the migration of neural crest cells, the major mesenchymal cell type in the nascent vertebrate head [28]. We thus speculate that the primordial Lectican may have functioned to promote mesenchymal histology and/or migratory behavior during development. In support of this scenario, development in invertebrate deuterostomes is largely, or completely epithelial. Indeed, the invertebrate with the most vertebrate-like body plan, amphioxus, develops without any discernible mesenchyme [100, 101]. Comprehensive analyses of *lectican* function in a wider range of vertebrates, including lamprey, using new methods for loss-of-function perturbation [102] should help test this hypothesis.

ACKNOWLEDGEMENTS

The authors thank Scott Miehls at the USGS Hammond Bay Biological Station for providing adult sea lampreys. They also thank Jeremiah J. Smith at the University of Kentucky, Jr-Kai Yu at the Academia Sinica in Taipei, Taiwan, as well as Juan Pascual-Anaya and Shigeru Kuratani at the RIKEN Institute in Kobe, Japan for supplemental transcriptomic data. Zachary Root, Marek Romasek, Tyler Square, David Jandzik, and Daniel Medeiros were supported by National Science Foundation grants IOS 1656843 and IOS 1257040 to Daniel Medeiros. Zachary Root, Cara Allen, and Margaux Brewer were also supported by the Beverly Sears and EBIO grants through the University of Colorado Boulder. David Jandzik was additionally supported by the Scientific Grant Agency of the Slovak Republic VEGA grant No.1/0415/17.

METHODS

Isolation of lamprey *lectican* homologues

Lamprey *lectican* sequences were assembled from transcriptomic reads of Tahara t. 26.5 embryos and late larval oral disc tissue that were previously gathered. Sequences from these files were used for our phylogenetic and syntenic analyses. For *in situ* hybridizations for *lecA*, primers were designed from lamprey genomic sequence to amplify conserved exon sequences, which were cloned into the pJet1.2 vector from ThermoFisher©. For *lecB, lecC,* and *lecD*, 500bp regions from transcriptomic sequences were selected and ordered as fragments in pUC57-amp vector from Synbio Tech©.

Phylogenetic Analysis

General Procedure

Peptide sequences of gnathostome genes were gathered on NCBI and aligned with lamprey genes using the PROBALIGN [71] program on CIPRES [73] servers. For all alignments, we used a gap open penalty of 20 and a gap extension penalty of 1. To determine the optimal substitution model for our phylogenetic analysis, we used ProtTest v3.4.2 [72]. For all tests, we

allowed the possibility of invariant sites, empirical frequencies, and we used a fixed BIONJ tree topology to determine our ideal model. For our phylogenetic analysis, we used maximum likelihood analyses using RAxML-HPC2 Workflow on CIPRES servers. Using the parameters recommended by ProtTest, our likelihood scores were bootstrapped with 1000 trees for each test to derive a consensus tree. Our consensus trees were lastly visualized using FigTree v1. 4.4 [74].

Lectican Orthology Tests

Due to the large amounts of evolutionary time passing since the divergence of lamprey and gnathostomes, we tested both large and small numbers of taxa per gene as well as the inclusion or exclusion of hagfish sequences using the aforementioned methods. The *lectican* N terminus shares sequence similarities with the *hapln* genes, so we next performed phylogenetic analyses using the N termini of these genes, vertebrate *hapln* genes, as well as X-Link-containing genes that have been identified outside of vertebrates. Lecticans have overall more sequence conservation at the N and C termini, so we lastly tested substitution models that were specific to each termini, additionally removing the intermediate domain for these phylogenetic analyses. For our original *lectican* test, a DCMut + I + G + F model was calculated with a log likelihood score of -80,905.555 under Akaike Information Criterion (AIC). For our HAPLN test, a JTT + G model was calculated with a log likelihood score of -29,806.183 under AIC. Our *lectican* + hagfish test yielded a VT + I + G + F model with a log likelihood score of -152,828.685 under AIC. Our *lectican* + hagfish test yielded a VT + I + G + F model with a log likelihood score of -152,828.685 under AIC. Our HAPLN + N terminus test yielded a WAG + G + F model with a log likelihood score of -37,630.993 under AIC. When testing specific domain models, a WAG + I + G + F model was calculated for the N terminus with a log likelihood score of -37,763.00 under AIC. Conversely, our C terminus yielded a JTT + I + G model with a log likelihood score of --

21.947.234 under AIC. Lastly, for our *mef2* test, a JTT+ G + F model was calculated with a log likelihood score of -18,094.435 under AIC.

Synteny Analysis

For our microsynteny analysis, we gathered peptide sequences of gnathostome *lecticans* on NCBI and found their respective genomic location using UCSC's Genome Browser and BLAT tool [103, 104] as well as ENSEMBL [105]. We then used sequences of elephant shark (*Callorhinchus milii*), dog (*Canis lupus familiaris*), chicken (*Gallus gallus*), mouse (*Mus musculus*), African clawed frog (*Xenopus tropicalis*), Spotted gar (*Lepisosteus ocullatus*), and human (*Homo sapiens*) to reconstruct the ancestral arrangement of genes around the *acan, bcan, ncan,* and *vcan* loci. To do this, we compared genes in the +/- 250-300kb around each gnathostome locus. Syntelogs conserved in six of the seven gnathostomes (or five of seven gnathostomes, if one of the five organisms was elephant shark, the most basally diverging gnathostome analyzed), were included in the reconstructed loci. The orientation of each syntelog was determined by the majority orientation. We then used UCSC's Genome Browser to identify all genes within +/- 400kb of each lamprey *lectican*. Because comparisons of the genes immediately adjacent to the gnathostome and lamprey *lectican* loci revealed very few conserved syntelogs [Fig. 2A], we expanded our analysis to include a larger selection of syntenic genes [Fig. S8]. To do this we identified the 20 genes (when available) immediately 5' and 3' of the *acan, ncan,* and *vcan* loci of three distantly related gnathostomes; chicken, elephant shark, and spotted gar. For *bcan*, which is not present in the current elephant shark genome assembly, we identified the 20 genes immediately 5' and 3' of the chicken, spotted gar, and zebrafish *bcan* loci. We then identified the 20 genes immediately 5' and 3' of lamprey *lecB and lecD*. For *lecC*, which sits near the 5' end of a scaffold, we identified the seven 5' genes, and the 33 3' genes. For *lecD,* which sits on a scaffold with less than 40 genes, all 29 flanking genes on the scaffold were used. For each gene identified as flanking a lamprey *lectican*, we then asked if there was

a syntelog near one or more gnathostome *lecticans*. We then color-coded the lamprey genes based on the gnathostome *lectican(s)* its syntelog is linked to [Fig. S8]

Embryo Collection and Staging.

Embryos for in situ hybridization were obtained from adult spawning-phase sea lampreys (Petromyzon marinus) collected from Lake Huron, MI, and kept in chilled holding tanks as previously described [9]. Embryos were staged according to the method of Tahara [75], fixed in MEMFA (Mops buffer, EGTA, MgSO4, and formaldehyde), rinsed in Mops buffer, dehydrated into methanol, and stored at –20 °C.

***In Situ* Hybridization.**

Riboprobes were made for anti-sense fragments using SP6 RNA Polymerase. Sequences for probes and genes are available upon request. In our experience, full-length P. marinus riboprobes, or riboprobes generated against untranslated regions of P. marinus transcripts, give higher background than short riboprobes against coding sequences. We believe that this is because lamprey noncoding sequences, especially 3′ UTRs, often have an excessive GC-repeat content, causing corresponding riboprobes to hybridize nonspecifically to off-targets. To mitigate this, we made short 500-bp riboprobes against coding regions and used a high-stringency hybridization protocol [95, 106]. Key parameters of this protocol include post-hybridization washes at 70 °C and the use of a low-salt, low-pH hybridization buffer (50% formamide; 1.3× SSC, pH 5.0; 5 mM EDTA, pH 8.0; 50 µg/mL tRNA; 0.2% Tween-20; 0.5% CHAPS; and 100 µg/mL heparin).

Histology and Sectioning

After in situ hybridization, embryos were postfixed in 4% paraformaldehyde/PBS (4 °C, overnight), rinsed in PBS, cryo-protected with 15% sucrose in water, embedded in 15%

492 sucrose, 7.5% gelatin/15% sucrose (37 °C, several hours to overnight), and 20% gelatin/15%
493 sucrose (37 °C overnight), frozen in -70 °C, and mounted with Tissue-Tek OCT compound
494 (Sakura Finetek). Cryo-sections of 10 µm were collected on Super Frost Plus slides (Fisher
495 Scientific), degelatinized in 3% gelatin in 38% ethanol, counterstained using Nuclear Fast Red
496 (Vector Laboratories), dried, and cover-slipped with DPX (Fluka) [107].
497
498 **Imaging**
499 Whole-mount in situ hybridized *P. marinus* embryos and larvae were photographed using a Carl
500 Zeiss Axiocam MRc5, Carl ZeissDiscovery V8 dissecting microscope, and Axiovision 4.6
501 software. Sections were photographed using a Carl Zeiss Imager A2 compound microscope.
502
503
504

REFERENCES

1. Gans, C. and R.G. Northcutt, *Neural crest and the origin of vertebrates: a new head.* Science, 1983. **220**(4594): p. 268-273.
2. Northcutt, R.G. and C. Gans, *The genesis of neural crest and epidermal placodes: a reinterpretation of vertebrate origins.* The Quarterly review of biology, 1983. **58**(1): p. 1-28.
3. Eames, B.F., D.M. Medeiros, and I. Adameyko, *Evolving Neural Crest Cells*. 2020: CRC Press.
4. Simakov, O., et al., *Deeply conserved synteny resolves early events in vertebrate evolution.* Nature Ecology & Evolution, 2020: p. 1-11.
5. Martinez-Morales, J.-R., et al., *New genes in the evolution of the neural crest differentiation program.* Genome biology, 2007. **8**(3): p. R36.
6. Braasch, I. and M. Schartl, *Evolution of endothelin receptors in vertebrates.* General and comparative endocrinology, 2014. **209**: p. 21-34.
7. Ohno, S., *Evolution by gene duplication*. 2013: Springer Science & Business Media.
8. Van de Peer, Y., S. Maere, and A. Meyer, *The evolutionary significance of ancient genome duplications.* Nature Reviews Genetics, 2009. **10**(10): p. 725-732.
9. Square TA, J.D., Masey JL, Romášek M, Stein HP, Hansen AW, Purkayastha A, Cattell MV, Medeiros DM, *Evolution of the Endothelin Pathway Drove Neural Crest Cell Diversification.* Nature, 2020. **(in press)**.
10. Sauka-Spengler, T., et al., *Ancient evolutionary origin of the neural crest gene regulatory network.* Developmental cell, 2007. **13**(3): p. 405-420.
11. Hockman, D., et al., *A genome-wide assessment of the ancestral neural crest gene regulatory network.* Nature communications, 2019. **10**(1): p. 1-15.
12. Marlétaz, F., et al., *Amphioxus functional genomics and the origins of vertebrate gene regulation.* Nature, 2018. **564**(7734): p. 64-70.
13. Meulemans, D. and M. Bronner-Fraser, *Gene-regulatory interactions in neural crest evolution and development.* Developmental cell, 2004. **7**(3): p. 291-299.
14. Meulemans, D. and M. Bronner-Fraser, *Central role of gene cooption in neural crest evolution.* Journal of Experimental Zoology Part B: Molecular and Developmental Evolution, 2005. **304**(4): p. 298-303.
15. Martik, M.L., et al., *Evolution of the new head by gradual acquisition of neural crest regulatory circuits.* Nature, 2019. **574**(7780): p. 675-678.
16. Kawashima, T., et al., *Domain shuffling and the evolution of vertebrates.* Genome research, 2009. **19**(8): p. 1393-1403.
17. Zelensky, A.N. and J.E. Gready, *The C-type lectin-like domain superfamily.* The FEBS journal, 2005. **272**(24): p. 6179-6217.
18. Spicer, A.P., A. Joo, and R.A. Bowling, *A Hyaluronan Binding Link Protein Gene Family Whose Members Are Physically Linked Adjacent to Chrondroitin Sulfate Proteoglycan Core Protein Genes THE MISSING LINKS.* Journal of Biological Chemistry, 2003. **278**(23): p. 21083-21091.
19. Wada, H., *Domain Shuffling and the Evolution of Vertebrate Extracellular Matrix*, in *Evolution of Extracellular Matrix*. 2013, Springer. p. 27-37.
20. Milev, P., et al., *Differential regulation of expression of hyaluronan-binding proteoglycans in developing brain: aggrecan, versican, neurocan, and brevican.* Biochemical and biophysical research communications, 1998. **247**(2): p. 207-212.
21. Miura, R., et al., *The proteoglycan lectin domain binds sulfated cell surface glycolipids and promotes cell adhesion.* Journal of Biological Chemistry, 1999. **274**(16): p. 11431-11438.

22. Mundlos, S., et al., *Distribution of cartilage proteoglycan (aggrecan) core protein and link protein gene expression during human skeletal development.* Matrix, 1991. **11**(5): p. 339-346.
23. Watanabe, H., Y. Yamada, and K. Kimata, *Roles of aggrecan, a large chondroitin sulfate proteoglycan, in cartilage structure and function.* The journal of biochemistry, 1998. **124**(4): p. 687-693.
24. Perris, R. and S. Johansson, *Inhibition of neural crest cell migration by aggregating chondroitin sulfate proteoglycans is mediated by their hyaluronan-binding region.* Developmental biology, 1990. **137**(1): p. 1-12.
25. Morawski, M., et al., *Aggrecan: beyond cartilage and into the brain.* The international journal of biochemistry & cell biology, 2012. **44**(5): p. 690-693.
26. Seidenbecher, C.I., et al., *Transcripts for secreted and GPI-anchored brevican are differentially distributed in rat brain.* European Journal of Neuroscience, 1998. **10**(5): p. 1621-1630.
27. Krueger, R., A. Hennig, and N. Schwartz, *Two immunologically and developmentally distinct chondroitin sulfate proteolglycans in embryonic chick brain.* Journal of Biological Chemistry, 1992. **267**(17): p. 12149-12161.
28. Perissinotto, D., et al., *Avian neural crest cell migration is diversely regulated by the two major hyaluronan-binding proteoglycans PG-M/versican and aggrecan.* Development, 2000. **127**(13): p. 2823-2842.
29. Zanin, M.K., et al., *Distinct spatial and temporal distributions of aggrecan and versican in the embryonic chick heart.* The Anatomical Record: An Official Publication of the American Association of Anatomists, 1999. **256**(4): p. 366-380.
30. Casini, P., et al., *Identification and gene expression of versican during early development of Xenopus.* International Journal of Developmental Biology, 2004. **52**(7): p. 993-918.
31. Landolt, R.M., et al., *Versican is selectively expressed in embryonic tissues that act as barriers to neural crest cell migration and axon outgrowth.* Development, 1995. **121**(8): p. 2303-2312.
32. Kang, J.S., et al., *Characterization of dermacan, a novel zebrafish lectican gene, expressed in dermal bones.* Mechanisms of development, 2004. **121**(3): p. 301-312.
33. Snow, H.E., et al., *Versican expression during skeletal/joint morphogenesis and patterning of muscle and nerve in the embryonic mouse limb.* The Anatomical Record Part A: Discoveries in Molecular, Cellular, and Evolutionary Biology: An Official Publication of the American Association of Anatomists, 2005. **282**(2): p. 95-105.
34. Henderson, D.J. and A.J. Copp, *Versican expression is associated with chamber specification, septation, and valvulogenesis in the developing mouse heart.* Circulation research, 1998. **83**(5): p. 523-532.
35. Oohashi, T., et al., *Bral1, a brain-specific link protein, colocalizing with the versican V2 isoform at the nodes of Ranvier in developing and adult mouse central nervous systems.* Molecular and Cellular Neuroscience, 2002. **19**(1): p. 43-57.
36. Courel, M.-N., et al., *Hyaluronectin is produced by oligodendrocytes and Schwann cells in vitro.* Journal of neurocytology, 1998. **27**(1): p. 27-32.
37. Bignami, A., G. Perides, and F. Rahemtulla, *Versican, a hyaluronate-binding proteoglycan of embryonal precartilaginous mesenchyma, is mainly expressed postnatally in rat brain.* Journal of neuroscience research, 1993. **34**(1): p. 97-106.
38. Szabó, A., et al., *Neural crest streaming as an emergent property of tissue interactions during morphogenesis.* PLoS computational biology, 2019. **15**(4): p. e1007002.
39. Frischknecht, R. and C.I. Seidenbecher, *Brevican: a key proteoglycan in the perisynaptic extracellular matrix of the brain.* The international journal of biochemistry & cell biology, 2012. **44**(7): p. 1051-1054.

40. Ogawa, T., et al., *Brevican in the developing hippocampal fimbria: differential expression in myelinating oligodendrocytes and adult astrocytes suggests a dual role for brevican in central nervous system fiber tract development.* Journal of Comparative Neurology, 2001. **432**(3): p. 285-295.
41. Gary, S.C., G.M. Kelly, and S. Hockfield, *BEHAB/brevican: a brain-specific lectican implicated in gliomas and glial cell motility.* Current opinion in neurobiology, 1998. **8**(5): p. 576-581.
42. Jaworski, D.M., G.M. Kelly, and S. Hockfield, *The CNS-specific hyaluronan-binding protein BEHAB is expressed in ventricular zones coincident with gliogenesis.* Journal of Neuroscience, 1995. **15**(2): p. 1352-1362.
43. Yamada, H., et al., *Molecular cloning of brevican, a novel brain proteoglycan of the aggrecan/versican family.* Journal of Biological Chemistry, 1994. **269**(13): p. 10119-10126.
44. Rauch, U., et al., *Cloning and primary structure of neurocan, a developmentally regulated, aggregating chondroitin sulfate proteoglycan of brain.* Journal of Biological Chemistry, 1992. **267**(27): p. 19536-19547.
45. Oohira, A., et al., *Developmentally regulated expression of a brain specific species of chondroitin sulfate proteoglycan, neurocan, identified with a monoclonal antibody 1G2 in the rat cerebrum.* Neuroscience, 1994. **60**(1): p. 145-157.
46. Georgadaki, K. and N. Zagris, *Neurocan developmental expression and function during early avian embryogenesis.* Research Journal of Developmental Biology, 2014. **1**(1).
47. Bell, G.W., T.A. Yatskievych, and P.B. Antin, *GEISHA, a whole-mount in situ hybridization gene expression screen in chicken embryos.* Developmental dynamics: an official publication of the American Association of Anatomists, 2004. **229**(3): p. 677-687.
48. Staudt, N., et al., *A panel of recombinant monoclonal antibodies against zebrafish neural receptors and secreted proteins suitable for wholemount immunostaining.* Biochemical and biophysical research communications, 2015. **456**(1): p. 527-533.
49. Owens, N.D., et al., *Measuring absolute RNA copy numbers at high temporal resolution reveals transcriptome kinetics in development.* Cell reports, 2016. **14**(3): p. 632-647.
50. Sander, V., J. Müllegger, and G. Lepperdinger, *Xenopus brevican is expressed in the notochord and the brain during early embryogenesis.* Mechanisms of development, 2001. **102**(1-2): p. 251-253.
51. Mishima, N. and S. Hoffman, *Neurocan in the embryonic avian heart and vasculature.* The Anatomical Record Part A: Discoveries in Molecular, Cellular, and Evolutionary Biology, 2003. **272**(2): p. 556-562.
52. Barnette, D.N., et al., *Tgfβ-Smad and MAPK signaling mediate scleraxis and proteoglycan expression in heart valves.* Journal of molecular and cellular cardiology, 2013. **65**: p. 137-146.
53. Mukhopadhyay, A., et al., *Erosive vitreoretinopathy and wagner disease are caused by intronic mutations in CSPG2/Versican that result in an imbalance of splice variants.* Investigative ophthalmology & visual science, 2006. **47**(8): p. 3565-3572.
54. Yamamura, H., et al., *A heart segmental defect in the anterior-posterior axis of a transgenic mutant mouse.* Developmental biology, 1997. **186**(1): p. 58-72.
55. Mjaatvedt, C., et al., *The Cspg2 gene, disrupted in the hdf mutant, is required for right cardiac chamber and endocardial cushion formation.* Developmental biology, 1998. **202**(1): p. 56-66.
56. Brakebusch, C., et al., *Brevican-deficient mice display impaired hippocampal CA1 long-term potentiation but show no obvious deficits in learning and memory.* Molecular and cellular biology, 2002. **22**(21): p. 7417-7427.
57. Zhou, X.-H., et al., *Neurocan is dispensable for brain development.* Molecular and Cellular Biology, 2001. **21**(17): p. 5970-5978.

58. Green, S.A. and M.E. Bronner, *The lamprey: a jawless vertebrate model system for examining origin of the neural crest and other vertebrate traits.* Differentiation, 2014. **87**(1-2): p. 44-51.
59. Nikitina, N., M. Bronner-Fraser, and T. Sauka-Spengler, *Microinjection of RNA and morpholino oligos into lamprey embryos.* Cold Spring Harbor protocols, 2009. **2009**(1): p. pdb. prot5123.
60. Oisi, Y., et al., *Craniofacial development of hagfishes and the evolution of vertebrates.* Nature, 2013. **493**(7431): p. 175-180.
61. Ota, K.G., S. Kuraku, and S. Kuratani, *Hagfish embryology with reference to the evolution of the neural crest.* Nature, 2007. **446**(7136): p. 672-675.
62. Shimeld, S.M. and P.C. Donoghue, *Evolutionary crossroads in developmental biology: cyclostomes (lamprey and hagfish).* Development, 2012. **139**(12): p. 2091-2099.
63. Forey, P. and P. Janvier, *Agnathans and the origin of jawed vertebrates.* Nature, 1993. **361**(6408): p. 129-134.
64. Delarbre, C., et al., *Complete mitochondrial DNA of the hagfish, Eptatretus burgeri: the comparative analysis of mitochondrial DNA sequences strongly supports the cyclostome monophyly.* Molecular phylogenetics and evolution, 2002. **22**(2): p. 184-192.
65. York, J.R. and D.W. McCauley, *The origin and evolution of vertebrate neural crest cells.* Open biology, 2020. **10**(1): p. 190285.
66. Square, T., et al., *The origin and diversification of the developmental mechanisms that pattern the vertebrate head skeleton.* Developmental biology, 2017. **427**(2): p. 219-229.
67. Murakami, Y., et al., *Evolution of the brain developmental plan: Insights from agnathans.* Developmental biology, 2005. **280**(2): p. 249-259.
68. Yang, X., Z. Si-Wei, and L. Qing-Wei, *Lamprey: a model for vertebrate evolutionary research.* Zoological research, 2016. **37**(5): p. 263.
69. York, J.R., E.M.-J. Lee, and D.W. McCauley, *The lamprey as a model vertebrate in evolutionary developmental biology*, in *Lampreys: Biology, Conservation and Control*. 2019, Springer. p. 481-526.
70. Smith, J.J., et al., *The sea lamprey germline genome provides insights into programmed genome rearrangement and vertebrate evolution.* Nature genetics, 2018. **50**(2): p. 270-277.
71. Roshan, U. and D.R. Livesay, *Probalign: multiple sequence alignment using partition function posterior probabilities.* Bioinformatics, 2006. **22**(22): p. 2715-2721.
72. Abascal, F., R. Zardoya, and D. Posada, *ProtTest: selection of best-fit models of protein evolution.* Bioinformatics, 2005. **21**(9): p. 2104-2105.
73. Miller, M.A., W. Pfeiffer, and T. Schwartz. *Creating the CIPRES Science Gateway for inference of large phylogenetic trees*. in *2010 gateway computing environments workshop (GCE)*. 2010. Ieee.
74. Rambaut, A., *FigTree v1. 4.4, a Graphical Viewer of Phylogenetic Trees. 2014. Java*. 2018.
75. Tahara, Y., *Normal stages of development in the lamprey, Lampetra reissneri (Dybowski).* Zoological science, 1988. **5**(1): p. 109-118.
76. Martin, W.M., L.A. Bumm, and D.W. McCauley, *Development of the viscerocranial skeleton during embryogenesis of the sea lamprey, Petromyzon Marinus.* Developmental Dynamics, 2009. **238**(12): p. 3126-3138.
77. McLysaght, A., K. Hokamp, and K.H. Wolfe, *Extensive genomic duplication during early chordate evolution.* Nature genetics, 2002. **31**(2): p. 200-204.
78. Dehal, P. and J.L. Boore, *Two rounds of whole genome duplication in the ancestral vertebrate.* PLoS biology, 2005. **3**(10).
79. Smith, J.J. and M.C. Keinath, *The sea lamprey meiotic map improves resolution of ancient vertebrate genome duplications.* Genome research, 2015. **25**(8): p. 1081-1090.

80. Guigo, R., I. Muchnik, and T.F. Smith, *Reconstruction of ancient molecular phylogeny.* Molecular phylogenetics and evolution, 1996. **6**(2): p. 189-213.
81. Kuraku, S., A. Meyer, and S. Kuratani, *Timing of genome duplications relative to the origin of the vertebrates: did cyclostomes diverge before or after?* Molecular biology and evolution, 2009. **26**(1): p. 47-59.
82. Rambeau, P., et al., *Reduced aggrecan expression affects cardiac outflow tract development in zebrafish and is associated with bicuspid aortic valve disease in humans.* International journal of cardiology, 2017. **249**: p. 340-343.
83. Schneider, A., *Anatomie und entwickelungsgeschichte von Petromyzon und ammocoetes.* Beitrage zur vergleichenden. Anatomie und Entwickelungsgeschichte der Wirbeltiere. Berlin: Reimer. p, 1879: p. 85-92.
84. Gaskell, W.H., *The origin of vertebrates*. 2019: Good Press.
85. Mangia, F. and G. Palladini, *Histochemical studies on the mucocartilage of the lamprey during its larval ontogenesis.* Archives d'anatomie microscopique et de morphologie experimentale, 1970. **59**(3): p. 283.
86. Wright, G.M. and J.H. Youson, *Ultrastructure of mucocartilage in the larval anadromous sea lamprey, Petromyzon marinus L.* American Journal of Anatomy, 1982. **165**(1): p. 39-51.
87. Armstrong, L., G.M. Wright, and J. Youson, *Transformation of mucocartilage to a definitive cartilage during metamorphosis in the sea lamprey, Petromyzon marinus.* Journal of morphology, 1987. **194**(1): p. 1-21.
88. Yao, T., et al., *Development of lamprey mucocartilage and its dorsal–ventral patterning by endothelin signaling, with insight into vertebrate jaw evolution.* Journal of Experimental Zoology Part B: Molecular and Developmental Evolution, 2011. **316**(5): p. 339-346.
89. Cattell, M., et al., *A new mechanistic scenario for the origin and evolution of vertebrate cartilage.* PloS one, 2011. **6**(7).
90. Ota, K.G. and S. Kuratani, *Expression pattern of two collagen type 2 α1 genes in the Japanese inshore hagfish (Eptatretus burgeri) with special reference to the evolution of cartilaginous tissue.* Journal of Experimental Zoology Part B: Molecular and Developmental Evolution, 2010. **314**(2): p. 157-165.
91. Ohtani, K., et al., *Expression of Sox and fibrillar collagen genes in lamprey larval chondrogenesis with implications for the evolution of vertebrate cartilage.* Journal of Experimental Zoology Part B: Molecular and Developmental Evolution, 2008. **310**(7): p. 596-607.
92. Parker, W.K., *On the skeleton of the marsipobranch fishes. Part I. The Myxinoids (Myxine, and Bdellostoma).* Philosophical Transactions of the Royal Society of London, 1883. **174**: p. 373-409.
93. Cole, F.J., *XXX.—A Monograph on the general Morphology of the Myxinoid Fishes, based on a study of Myxine. Part I. The Anatomy of the Skeleton.* Earth and Environmental Science Transactions of The Royal Society of Edinburgh, 1906. **41**(3): p. 749-788.
94. Fujimoto, S., et al., *Non-parsimonious evolution of hagfish Dlx genes.* BMC evolutionary biology, 2013. **13**(1): p. 15.
95. Cerny, R., et al., *Evidence for the prepattern/cooption model of vertebrate jaw evolution.* Proceedings of the National Academy of Sciences, 2010. **107**(40): p. 17262-17267.
96. Medeiros, D.M. and J.G. Crump, *New perspectives on pharyngeal dorsoventral patterning in development and evolution of the vertebrate jaw.* Developmental biology, 2012. **371**(2): p. 121-135.

97. Takio, Y., et al., *Hox gene expression patterns in Lethenteron japonicum embryos—insights into the evolution of the vertebrate Hox code.* Developmental biology, 2007. **308**(2): p. 606-620.
98. Force, A., et al., *Preservation of duplicate genes by complementary, degenerative mutations.* Genetics, 1999. **151**(4): p. 1531-1545.
99. Jandzik, D., et al., *Evolution of the new vertebrate head by co-option of an ancient chordate skeletal tissue.* Nature, 2015. **518**(7540): p. 534-537.
100. Conklin, E.G., *The embryology of amphioxus.* Journal of Morphology, 1932. **54**(1): p. 69-151.
101. Carvalho, J.E., et al., *An updated staging system for cephalochordate development: one table suits them all.* bioRxiv, 2020.
102. Square, T., et al., *CRISPR/Cas9-mediated mutagenesis in the sea lamprey Petromyzon marinus: a powerful tool for understanding ancestral gene functions in vertebrates.* Development, 2015. **142**(23): p. 4180-4187.
103. Kent, W.J., et al., *The human genome browser at UCSC.* Genome research, 2002. **12**(6): p. 996-1006.
104. Kent, W.J., *BLAT—the BLAST-like alignment tool.* Genome research, 2002. **12**(4): p. 656-664.
105. Yates, A.D., et al., *Ensembl 2020.* Nucleic acids research, 2020. **48**(D1): p. D682-D688.
106. Square, T., et al., *Embryonic expression of endothelins and their receptors in lamprey and frog reveals stem vertebrate origins of complex Endothelin signaling.* Scientific reports, 2016. **6**(1): p. 1-13.
107. Jandzik, D., et al., *Roles for FGF in lamprey pharyngeal pouch formation and skeletogenesis highlight ancestral functions in the vertebrate head.* Development, 2014. **141**(3): p. 629-638.

FIGURE LEGENDS

Figure 1. Structural comparison and molecular phylogeny of vertebrate lecticans. (A) Domain structure of vertebrate Lecticans with the N-terminus to the left. **Keywords:** Ig: Immunoglobulin-like domain; G1 / G2: link domains; EGF: EGF-like domains; CRD: carbohydrate recognition domains; CCP: complement control protein domain. (B) Phylogenetic relationships of vertebrate Lecticans based on amino acid sequence alignments. Lamprey sequences are in gray boxes while individual gnathostome paralogy groups are in colored boxes. Maximum likelihood analysis scores are shown at the respective node. HAPLN1 sequences were designated as outgroup. Original tree and accession numbers for all sequences can be found in Fig. S1 and Tab. S1.

Figure 2. Summary of *lectican* microsynteny and implications for their evolutionary relationships. (A) Conserved genes adjacent to the gnathostome (top four) and lamprey (bottom four) lectican loci. Syntelogs are shown in orientation with respect to their linked *lectican* gene. *Lectican*s are in red. Homologous genes are colored the same. Gnathostome genes were surveyed within a 300kb radius while lamprey genes were surveyed within a 400kb radius. Macrosyntenic analyses can be found in Table S1. (B) Hypothetical scenarios for the evolution of vertebrate lecticans when synteny data is incorporated. While syntenic analyses suggest that *lecticanA* is orthologous to the *aggrecan*/*brevican* gene family, the relationship of *lecticanB*, *lecticanC*, or *lecticanD* is unclear.

Figure 3. Expression of *lecA* in embryos and larvae. Left lateral view in all non-prime panels. Developmental stage (Tahara, 1988) for each whole mount panel is in the bottom right corner. Prime panel stages correspond to their whole mount. For all non-prime panels, scale bar represents 500 **µ**m (A-B) *lecA* is expressed in the neural tube and presumptive somites (C-C') *lecA* is expressed in the myocardium of the heart, the notochord, neural tube floor plate, and

809 medial sclerotome. (D,D',D") *lecA* expression is in the pre-oral mesenchyme, the dorsal aspect
810 of the nascent pharyngeal arches, the otic vesicle, and the developing heart and brain
811 (E, E', E") *lecA* is expressed in the the premandibular mesenchyme, the dorsal sclerotome
812 lateral to the neural tube, pharyngeal neural crest cells, and developing heart tube. (F, H) *lecA* is
813 localized in the developing head skeleton as well as fin mesenchyme, but is absent from the
814 brain by this stage. (G, I) *lecA* expression is in the oral hood and velar mucocartilage as well as
815 fin mesenchyme. (H-I) Focused view of *lecA* expression in the developing fin. **Keywords:**
816 cncc's: cranial neural crest cells; he: heart; ht: heart tube; mc: myocardium; me: pre-oral
817 mesenchyme; nc: notochord; nt: neural tube; oh: oral hood; ov: otic vesicle; pa's: pharyngeal
818 arches; pll: posterior lateral line ganglion; sc: sclerotome; te: telencephalon; v: velum; zli: zona
819 limitans intrathalamica
820 **Figure 4.** Expression summary for *lecticanB* in *P. marinus* embryos. Left lateral view in all non-
821 prime panels. Developmental stage (Tahara, 1988) for each whole mount panel is in the bottom
822 right corner. Prime panel stages correspond to their whole mount. For all non-prime panels,
823 scale bar represents 500 **µ**m. (A-A') *lecB* expression is in the oral ectoderm (B-B') *lecB*
824 expression is in the oral ectoderm, lateral neural tube, and medial sclerotome (C,D,D') *lecB*
825 expression is in the developing brain, neural placodes, and pronephros. (E,E') *lecB* expression
826 is in the pharyngeal endoderm as well as the mucocartilage of the lateral velum and lower lip.
827 (F,F') *lecB* expression is in the mucocartilage of the ventrolateral pharyngeal bars and lower lip
828 as well as the oral papillae. **Keywords:** blh: basolateral hypothalamus; ll: lower lip; lp: lens
829 placode; mp: maxillomandibular placode; np: nasohypophyseal placode; nt: neural tube; oe: oral
830 ectoderm; op: ophthalmic placode; or: oral papillae; pe: pharyngeal endoderm; pr: pronephros;
831 sc: sclerotome; so: somites; v: velum; vpb: ventrolateral pharyngeal bars
832
833 **Figure 5.** Expression summary for *lecticanC* in *P. marinus* embryos. Left lateral view in all non-
834 prime panels. Developmental stage (Tahara, 1988) for each whole mount panel is in the bottom

right corner. Prime panel stages correspond to their whole mount. For all non-prime panels, scale bar represents 500 μm. (A-B) *lecC* is found in the cell-rich hyaline cartilage of the pharynx. (C) *lecC* is in the pharyngeal hyaline cartilage, the epitrematic and hypotrematic processes of the pharynx, as well as the trabeculae. **Keywords:** ep: epitrematic process; hc: hyaline cartilage; hp: hypotrematic process

Figure 6. Expression summary for *lecticanD* in *P. marinus* embryos. Left lateral view in all non-prime panels. Developmental stage (Tahara, 1988) for each whole mount panel is in the bottom right corner. Prime panel stages correspond to their whole mount. For panels A-C, scale bar represents 250 μm. For panels D-G, scale bar represents 500 μm (A) *lecD* is found in the somites. (B-B') *lecD* is additionally found in the first pharyngeal arch as well as the sclerotome and developing splanchnic mesoderm of the heart. (C) *lecD* expression ablates in the somites but continues in the first pharyngeal arch as well as the developing heart. (D-D') *lecD* is localized in the first pharyngeal arch, the heart tube, endocardium, and splanchnic mesoderm. (E) *lecD* is expressed in the developing aortic arches. (F) *lecD* expression is in the pharyngeal vasculature as well as the mucocartilage of the ventral pharynx. (G) lecD is expressed in the ventral aorta as well as the mucocartilage of the lower lip. **Keywords:** aa: aortic arches; ec: endocardium; he: heart; ht: heart tube; ll: lower lip mucocartilage; pa: first pharyngeal arch; sc: sclerotome; sm: splanchnic mesoderm; so: somites; va: ventral aorta; vp: ventral pharynx mucocartilage

Figure 7. The evolution of *lectican* expression patterns in the head. Modern gnathostome lectican expression is depicted based on current data for zebrafish (*Danio rerio*), frog (*Xenopus laevis*), chicken (*Gallus gallus*), and mouse (*Mus musculus*), and their "average" is depicted as an idealized proto-gnathostome. Expression data for chondrichthyans is currently not available.

Keywords: br: brain; he: heart; nc: notochord; nt: neural tube; ov: otic vesicle; sc: sclerotome; sk: skeletal mesenchyme

Figure S1. Phylogenetic tree built from lectican sequences in vertebrates with a larger number of taxa per gene as well as hagfish sequences. Maximum likelihood analysis scores are shown at the respective node. HAPLN1 sequences were designated as outgroup. Accession numbers for all sequences can be found in Tab. S1.

Figure S2. Phylogenetic tree built from lectican N-terminus sequences in vertebrates with a larger number of taxa per gene, hagfish N-terminus sequences, HAPLN genes, as well as X-link-containing genes outside of vertebrates. Maximum likelihood analysis scores are shown at the respective node. CD44 sequences were designated as outgroup. Accession numbers for all sequences can be found in Tab. S2.

Figure S3. Phylogenetic tree built from lectican N+C termini sequences in gnathostomes and lamprey with minimal taxa and using the substitution model determined from the N-terminus. HAPLN1 sequences were designated as outgroup. Accession numbers for all sequences can be found in Tab. S3.

Figure S4. Phylogenetic tree built from lectican N+C termini sequences in gnathostomes and lamprey with minimal taxa and using the substitution model determined from the C-terminus. HAPLN1 sequences were designated as outgroup. Accession numbers for all sequences can be found in Tab. S3.

Figure S5. Final phylogenetic tree built from LECTICAN sequences in gnathostomes and lamprey. Maximum likelihood analysis scores are shown at the respective node. HAPLN1

886 sequences were designated as outgroup. Accession numbers for all sequences can be found in
887 Tab. S4.
888
889 **Figure S6.** Phylogenetic tree reconstruction built from HAPLN sequences in gnathostomes and
890 lamprey. Maximum likelihood analysis scores are shown at the respective node. CD44
891 sequences were designated as outgroup. Accession numbers for all sequences can be found in
892 Tab. S5.
893
894 **Figure S7.** Phylogenetic tree reconstruction built from *MEF2* sequences in gnathostomes and
895 lamprey. Maximum likelihood analysis scores are shown at the respective node. Sox9
896 sequences were designated as outgroup. Accession numbers for all sequences can be found in
897 Tab. S6.
898
899 **Figure S8.** Comparison of genes syntenic to lamprey and gnathostome *lecticans*. Lamprey
900 genes are color-coded based on the *lectican* their gnathostome syntelog is linked to. Red
901 indicates the lamprey gene has a gnathostome homolog linked to *acan* only. Yellow indicates
902 the lamprey gene has a gnathostome homolog linked to *bcan* only. Blue indicates the lamprey
903 gene has a gnathostome homolog linked to *ncan* only. Green indicates the lamprey gene has a
904 gnathostome homolog linked to *vcan* only. Orange indicates the lamprey gene has a
905 gnathostome homolog linked to both *acan* and *bcan*. Turquoise indicates the lamprey gene has
906 a gnathostome homolog linked to both *ncan* and *vcan*. Gray indicates the lamprey gene has
907 gnathostome homologs linked to members of both the *acan*+*bcan* and *ncan*+*vcan* paralogy
908 groups. Light yellow indicates lamprey genes with homologs linked to multiple lamprey
909 *lecticans*. *LecA* is linked to 15 genes with gnathostome homologs linked exclusively to *acan*
910 and/or *bcan*, but only 4 linked exclusively to *ncan* and/or *vcan*. The ratios of exclusive *acan*

911 and/or *bcan* syntelogs to exclusive *ncan* and/or *vcan* syntelogs for *lecB*, *lecC*, and, *lecD* are 4:4,

912 8:7, and 8:5, respectively.

913

914

915

Figure 1

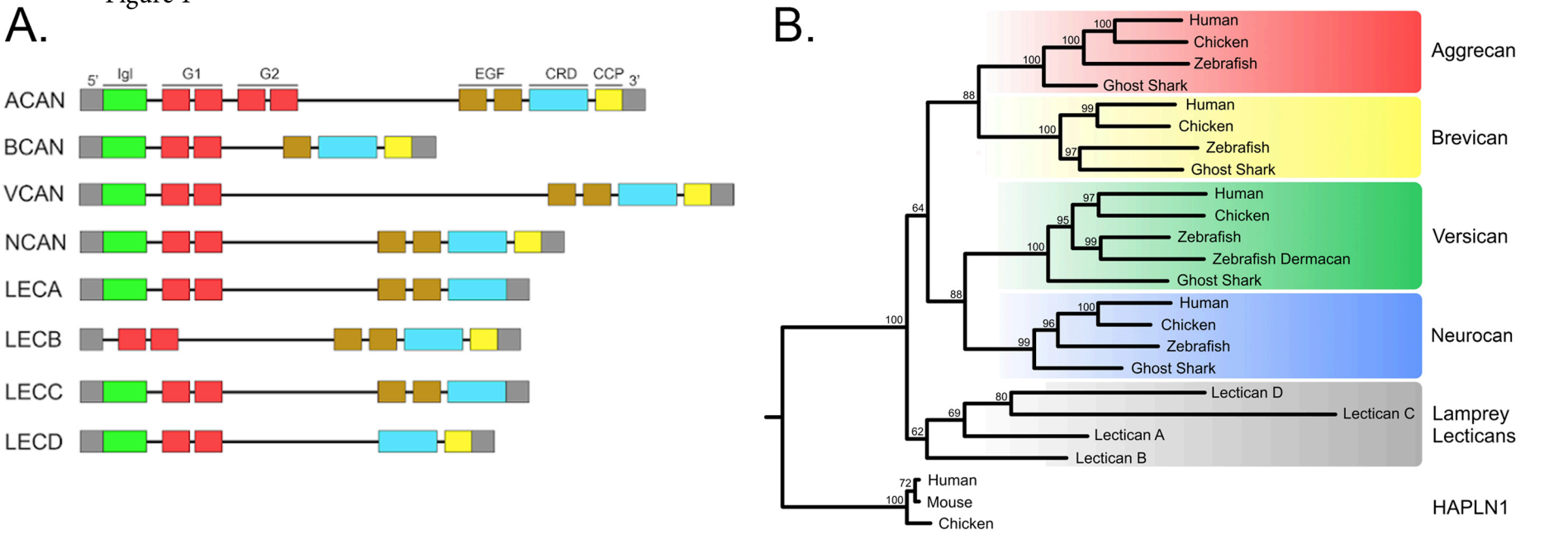
A.
5'
IgI
G1
G2
EGF
CRD
CCP
3'
ACAN
BCAN
VCAN
NCAN
LECA
LECB
LECC
LECD
B.
Human
Chicken
Zebrafish
Ghost Shark
Aggrecan
Human
Chicken
Zebrafish
Ghost Shark
Brevican
Human
Chicken
Zebrafish
Zebrafish Dermacan
Ghost Shark
Versican
Human
Chicken
Zebrafish
Ghost Shark
Neurocan
Lectican D
Lectican C
Lectican A
Lectican B
Lamprey Lecticans
Human
Mouse
Chicken
HAPLN1

Figure 2

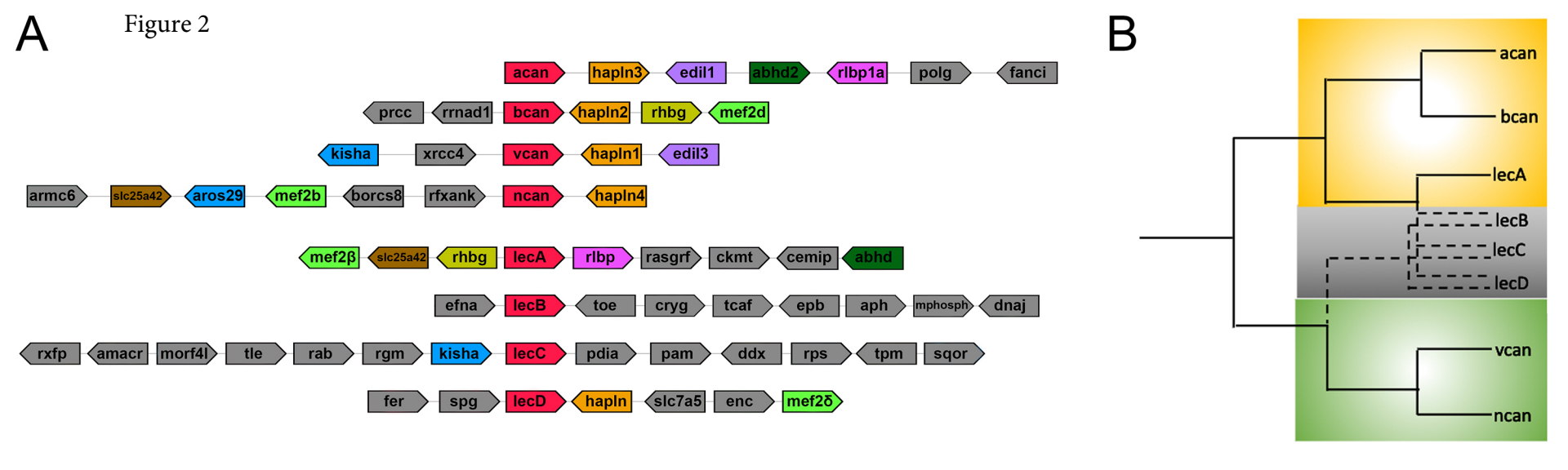
A
acan
hapln3
edil1
abhd2
rlbp1a
polg
fanci
prcc
rrnad1
bcan
hapln2
rhbg
mef2d
kisha
xrcc4
vcan
hapln1
edil3
armc6
slc25a42
aros29
mef2b
borcs8
rfxank
ncan
hapln4
mef2β
slc25a42
rhbg
lecA
rlbp
rasgrf
ckmt
cemip
abhd
efna
lecB
toe
cryg
tcaf
epb
aph
mphosph
dnaj
rxfp
amacr
morf4l
tle
rab
rgm
kisha
lecC
pdia
pam
ddx
rps
tpm
sqor
fer
spg
lecD
hapln
slc7a5
enc
mef2δ
B
acan
bcan
lecA
lecB
lecC
lecD
vcan
ncan

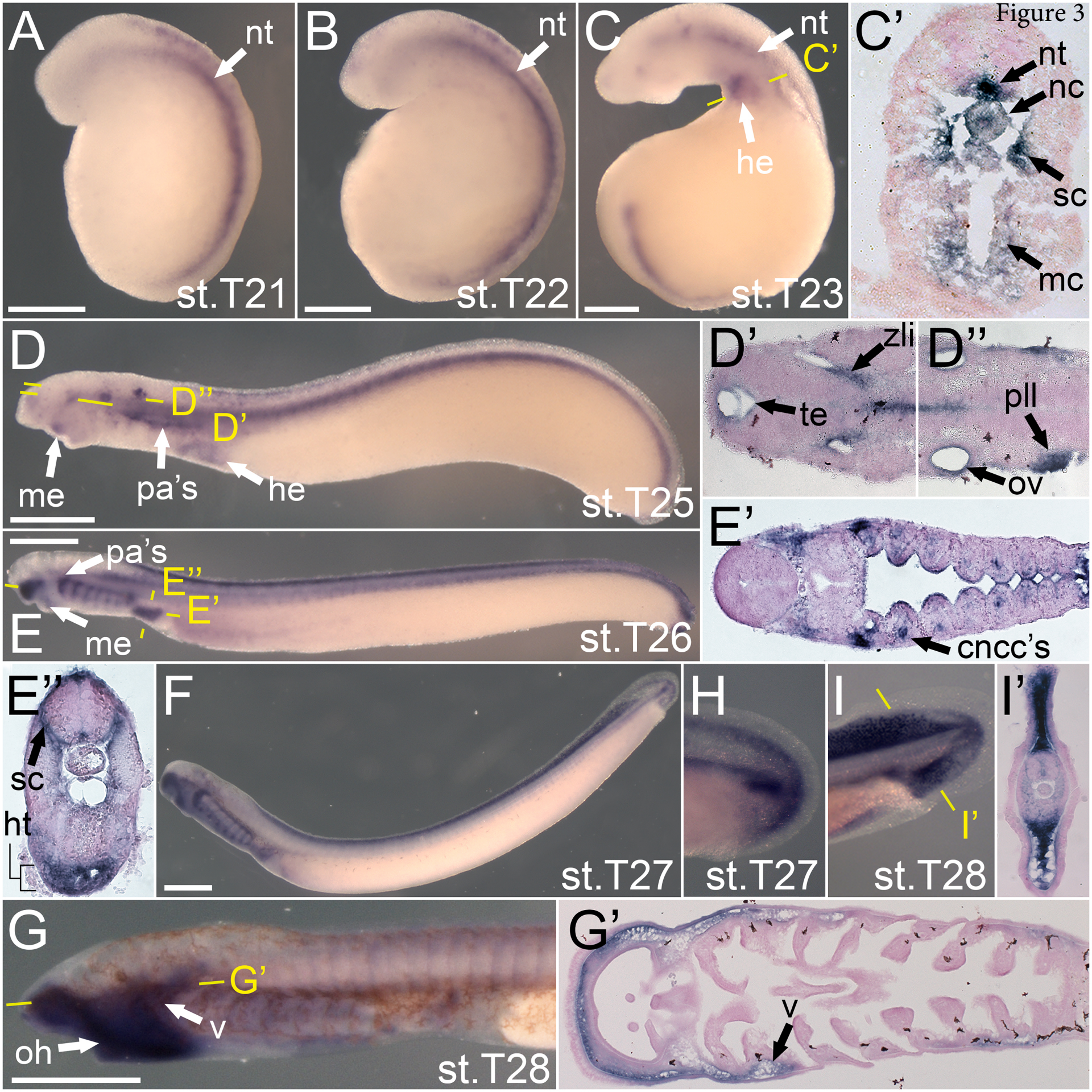
A
nt
st.T21
B
nt
st.T22
C
nt
C'
he
st.T23
C'
nt
nc
sc
mc
D
D''
D'
me
pa's
he
st.T25
D'
zli
te
D''
pll
ov
E
pa's
E''
E'
me
st.T26
E'
cncc's
E''
sc
ht
F
st.T27
H
st.T27
I
I'
st.T28
I'
G
G'
v
oh
st.T28
G'
v

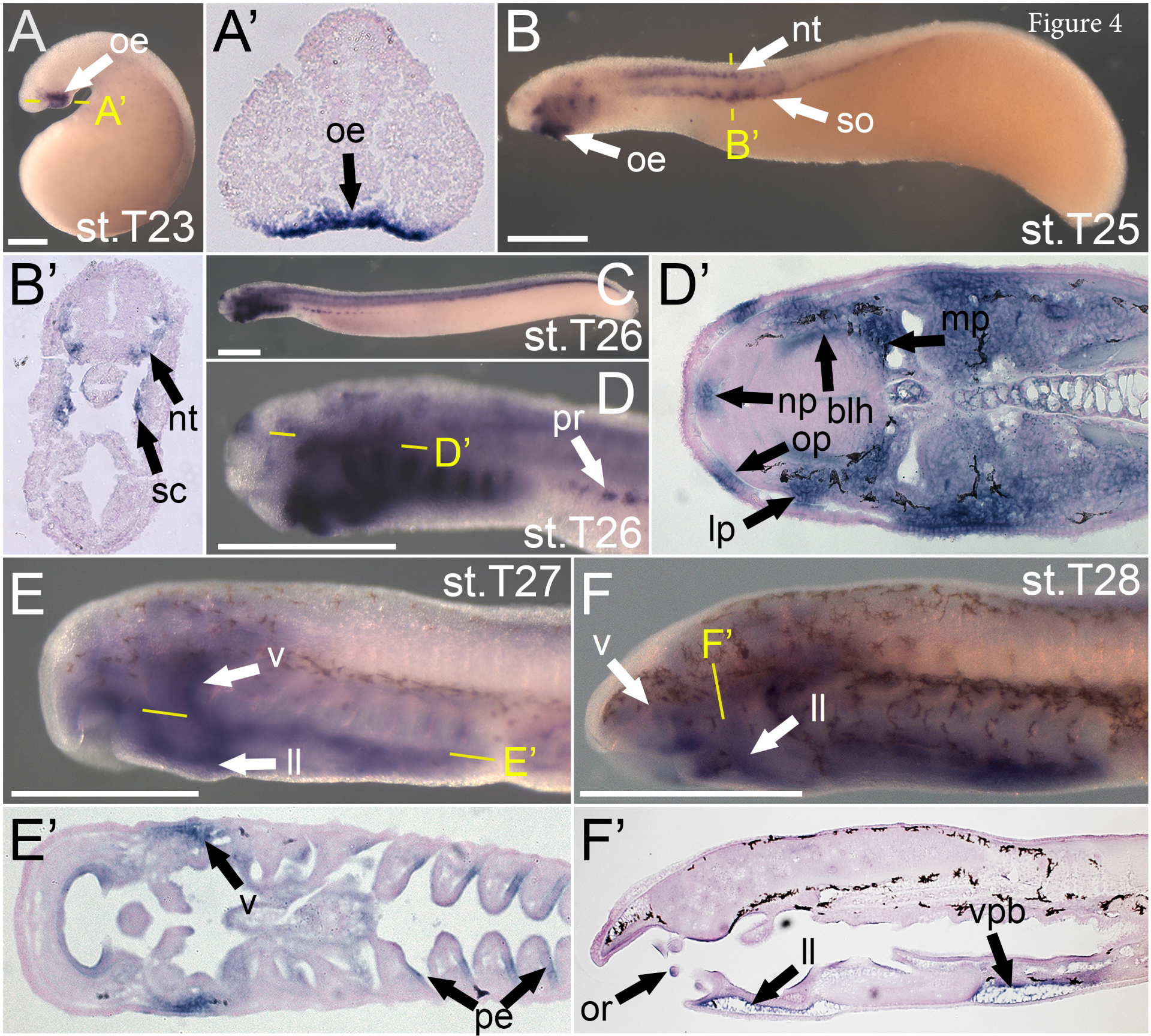
A
oe
A'
st.T23
A'
oe
B
nt
so
B'
oe
st.T25
Figure 4
B'
nt
sc
C
st.T26
D
pr
D'
st.T26
D'
mp
np
blh
op
lp
E
st.T27
v
ll
E'
F
st.T28
v
F'
ll
E'
v
pe
F'
vpb
ll
or

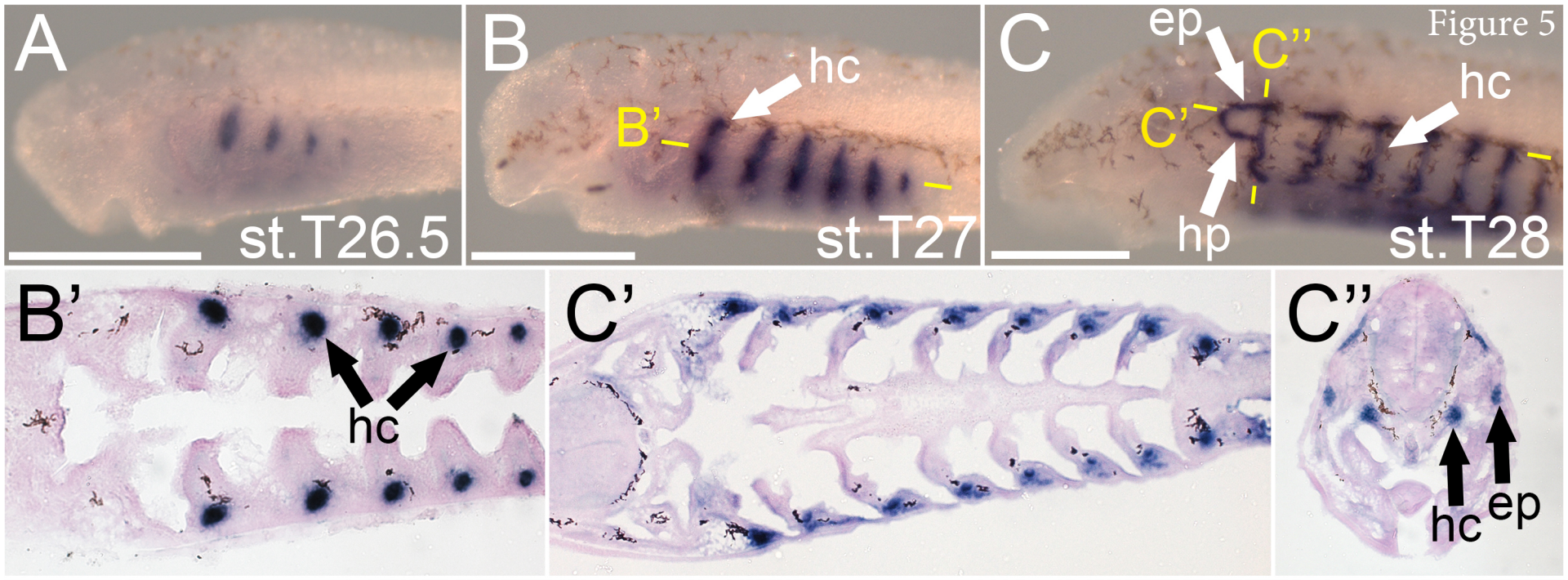
A
st.T26.5
B
hc
B'
st.T27
C
ep
C''
C'
hc
hp
st.T28
B'
hc
C'
C''
hc
ep

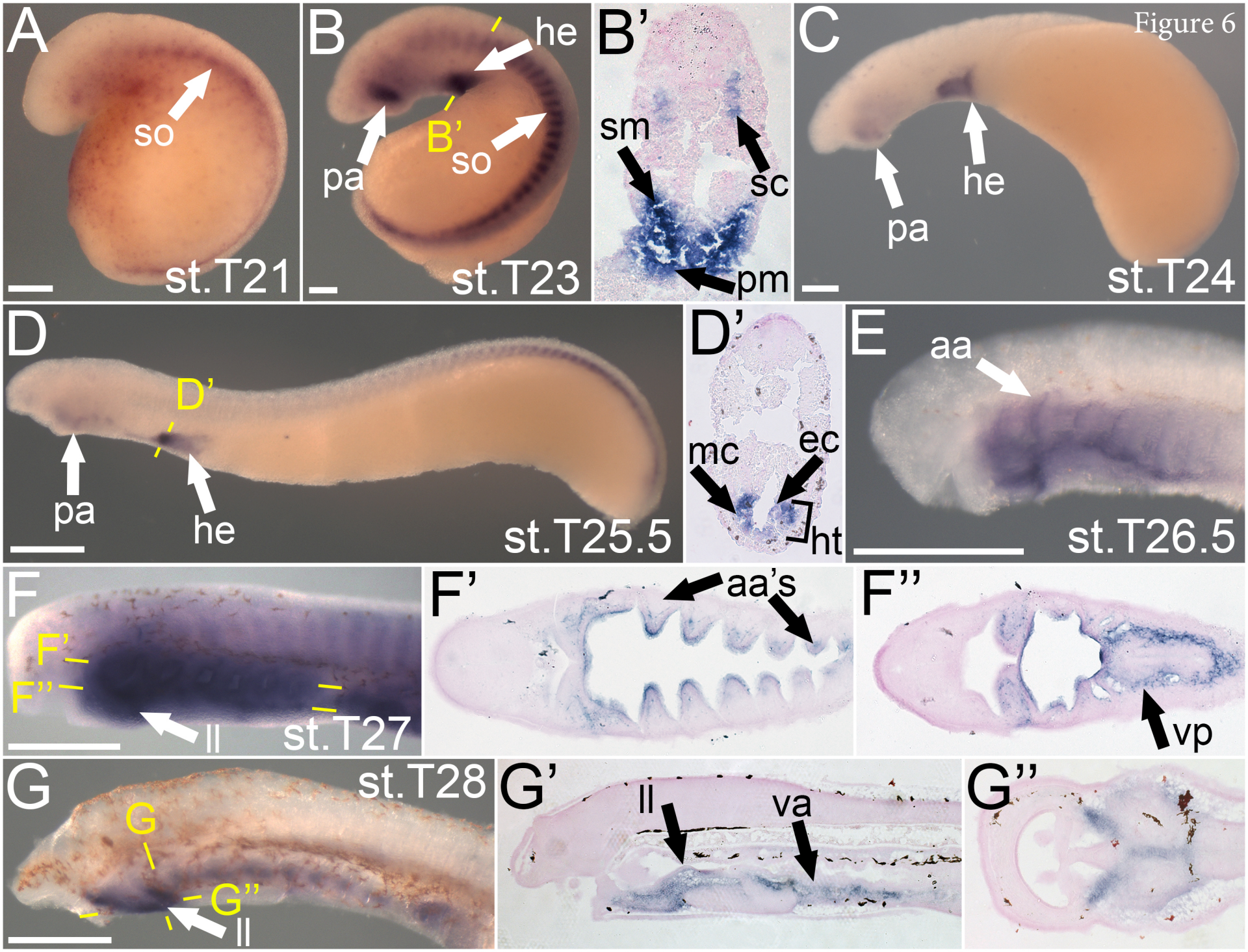
A
so
st.T21
B
he
B'
so
pa
st.T23
B'
sm
sc
pm
C
he
pa
st.T24
D
D'
pa
he
st.T25.5
D'
mc
ec
ht
E
aa
st.T26.5
F
F'
F''
II
st.T27
F'
aa's
F''
vp
G
st.T28
G
G''
II
G'
II
va
G''

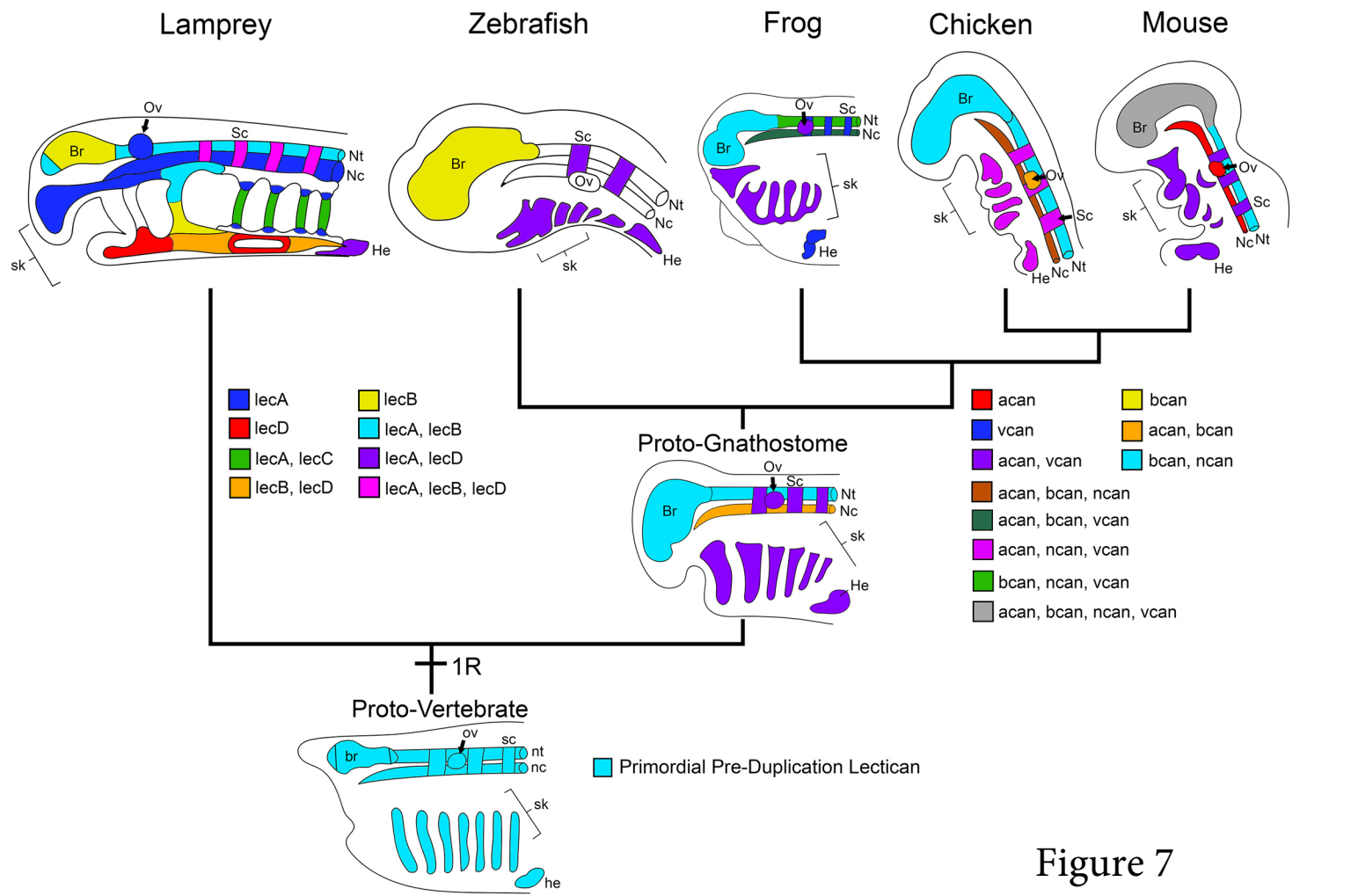
Lamprey
Zebrafish
Frog
Chicken
Mouse
Ov
Sc
Br
Nt
Nc
He
sk
lecA
lecB
lecD
lecA, lecB
lecA, lecC
lecA, lecD
lecB, lecD
lecA, lecB, lecD
Proto-Gnathostome
acan
bcan
vcan
acan, bcan
acan, vcan
bcan, ncan
acan, bcan, ncan
acan, bcan, vcan
acan, ncan, vcan
bcan, ncan, vcan
acan, bcan, ncan, vcan
1R
Proto-Vertebrate
ov
sc
br
nt
nc
he
Primordial Pre-Duplication Lectican

Figure 7

Table 1. Lecticans are mainly expressed in cells and tissues that are unique to vertebrates, or have distinct histology in vertebrates.

	Anterior Mesoderm and/or Cranial Neural Crest			**Axial Mesoderm**	**Paraxial Mesoderm**		**Intermed. Meso.**	**Lateral plate Mesoderm**		**Oropharyngeal Epithelia**		**Neural**	
	Cell-rich hyaline cartilage	ECM-rich hyaline cartilage	Muco-cartilage	Notochord	Fin Mes.	Sclero-tome	Pro-nephros	Somatic	Cardiac	Phar. endoderm	Oral ectoderm	CNS neurons	PNS neurons
Gnathostomes	*acan vcan*	*acan vcan*	N/A	*acan bcan*	*acan*	*acan vcan*	*vcan*	*acan vcan*	*vcan*	*vcan*	*bcan*	*bcan ncan*	*bcan ncan vcan*
Lamprey	*lecC lecA*	*?*	*lecA lecB lecD*	*lecA*	*lecA*	*lecA lecB*	*lecB*	No *lec*	*lecA lecD*	*lecB*	*lecB*	*lecA lecB*	*lecA lecB*
Urochordate	N/A	N/A	N/A	Present	N/A	N/A	N/A	N/A	Present	Present	Present	Present	Present
Cephalochordate	Present	N/A	N/A	Present	Present	Present	?	Present	N/A	Present	Present	Present	Present
Cell/tissue is unique to vertebrates?	**No**	**Yes**	**Yes**	**No**	**No**	**No**	**Yes[4]**	**No**	**No**	**No**	**No**	**No**	**No**
Cell/tissue has distinct histology in vertebrates?	**Yes[1]**	**-**	**-**	**No**	**Yes[2]**	**Yes[3]**	**-**	**Yes[5]**	**No**	**No**	**No**	**No**	**Yes[6]**

1. Unlike amphioxus cell-rich hyaline cartilage, vertebrate cell-rich hyaline cartilage develops from mesenchymal cells and can differentiate into ECM-rich hyaline cartilage
2. Amphioxus fin box mesoderm is epithelial and forms connective tissue, while vertebrate fin mesoderm delaminates and migrates as mesenchyme and can form cartilage and bone.
3. Amphioxus sclerotome is epithelial and forms connective tissue, while vertebrate sclerotome cells delaminate and migrate as mesenchyme and form cartilage and bone
4. Amphioxus nephridia and the vertebrate kidney consist of different cell types with no clear evolutionary relationship. The vertebrate kidney forms from migratory mesenchymal cells.
5. The amphioxus homolog of somatic LPM is epithelial and forms connective tissue, while gnathostome LPM cells delaminate and migrate as mesenchyme and form cartilage and bone in the limbs.
6. The PNS neurons of invertebrate chordates migrate short distances as neuroblasts, vertebrate PNS neurons migrate as multipotent mesenchymal cells that aggregate to form ganglia.

Figure S1

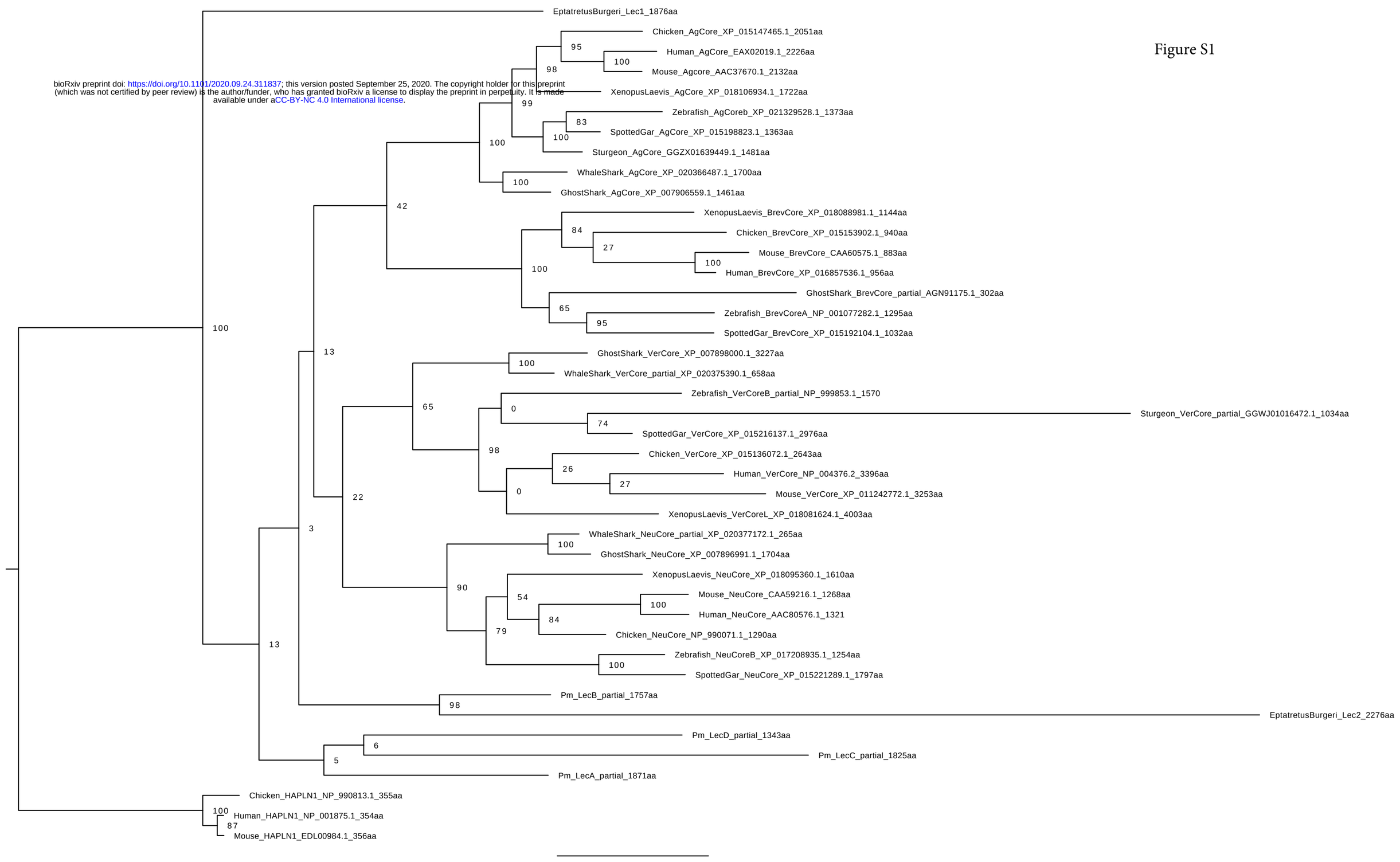

Figure S2

Figure S3

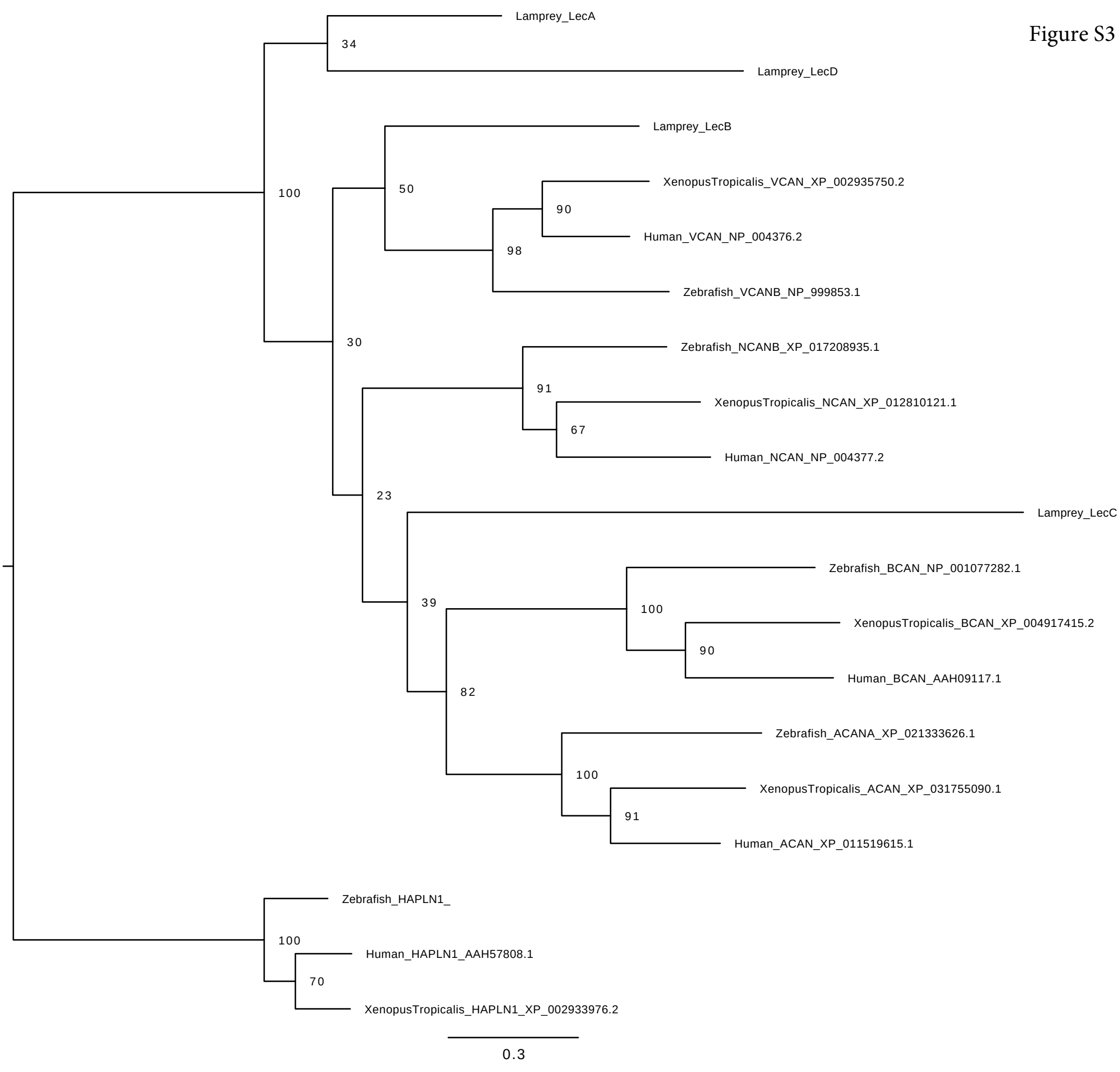
Lamprey_LecA
34
Lamprey_LecD
Lamprey_LecB
100
50
XenopusTropicalis_VCAN_XP_002935750.2
90
Human_VCAN_NP_004376.2
98
Zebrafish_VCANB_NP_999853.1
30
Zebrafish_NCANB_XP_017208935.1
91
XenopusTropicalis_NCAN_XP_012810121.1
67
Human_NCAN_NP_004377.2
23
Lamprey_LecC
Zebrafish_BCAN_NP_001077282.1
39
100
XenopusTropicalis_BCAN_XP_004917415.2
90
Human_BCAN_AAH09117.1
82
Zebrafish_ACANA_XP_021333626.1
100
XenopusTropicalis_ACAN_XP_031755090.1
91
Human_ACAN_XP_011519615.1
Zebrafish_HAPLN1_
100
Human_HAPLN1_AAH57808.1
70
XenopusTropicalis_HAPLN1_XP_002933976.2
0.3

Figure S4

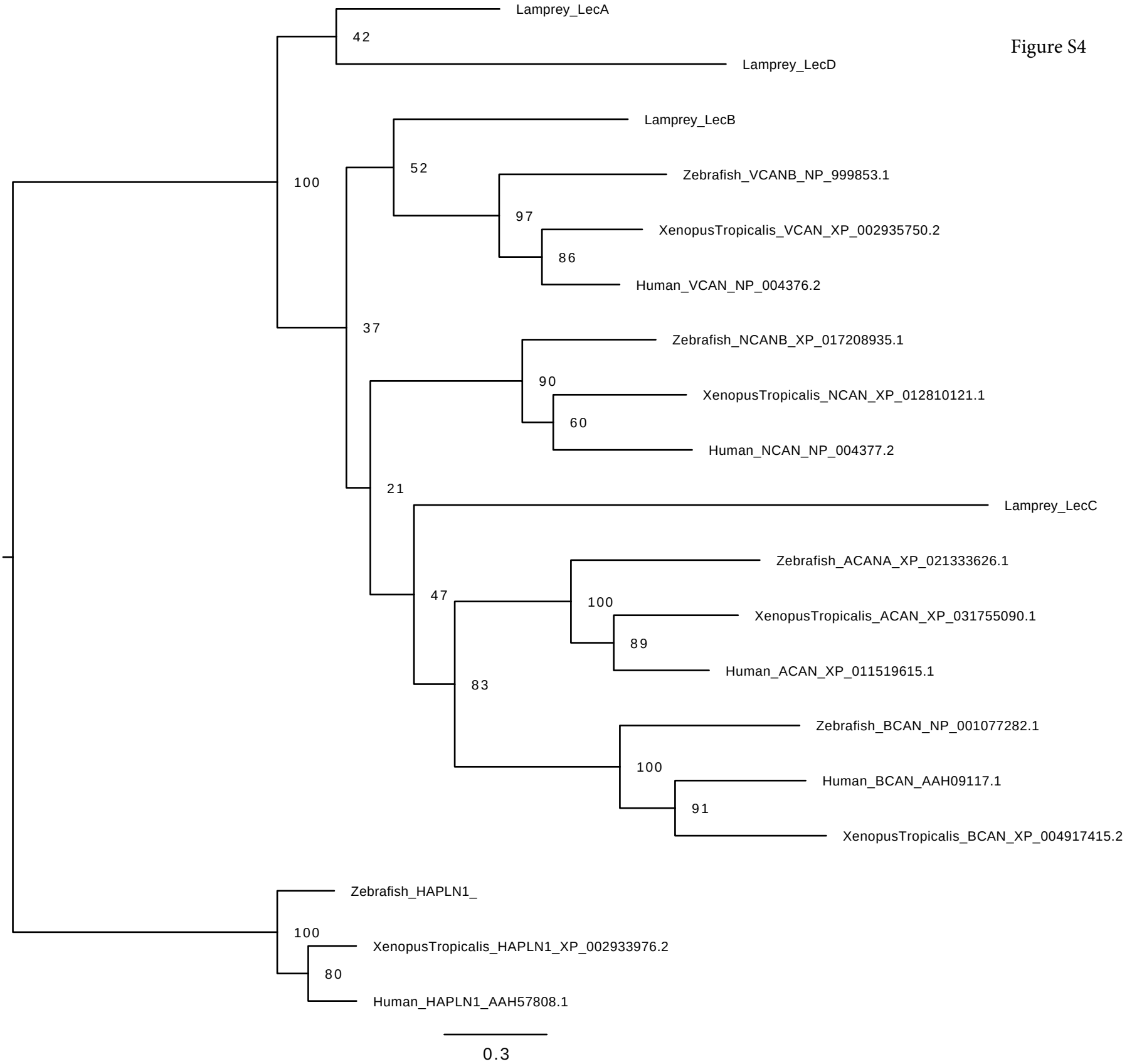
Lamprey_LecA
42
Lamprey_LecD
Lamprey_LecB
52
Zebrafish_VCANB_NP_999853.1
100
97
XenopusTropicalis_VCAN_XP_002935750.2
86
Human_VCAN_NP_004376.2
37
Zebrafish_NCANB_XP_017208935.1
90
XenopusTropicalis_NCAN_XP_012810121.1
60
Human_NCAN_NP_004377.2
21
Lamprey_LecC
Zebrafish_ACANA_XP_021333626.1
47
100
XenopusTropicalis_ACAN_XP_031755090.1
89
Human_ACAN_XP_011519615.1
83
Zebrafish_BCAN_NP_001077282.1
100
Human_BCAN_AAH09117.1
91
XenopusTropicalis_BCAN_XP_004917415.2
Zebrafish_HAPLN1_
100
XenopusTropicalis_HAPLN1_XP_002933976.2
80
Human_HAPLN1_AAH57808.1
0.3

Figure S5

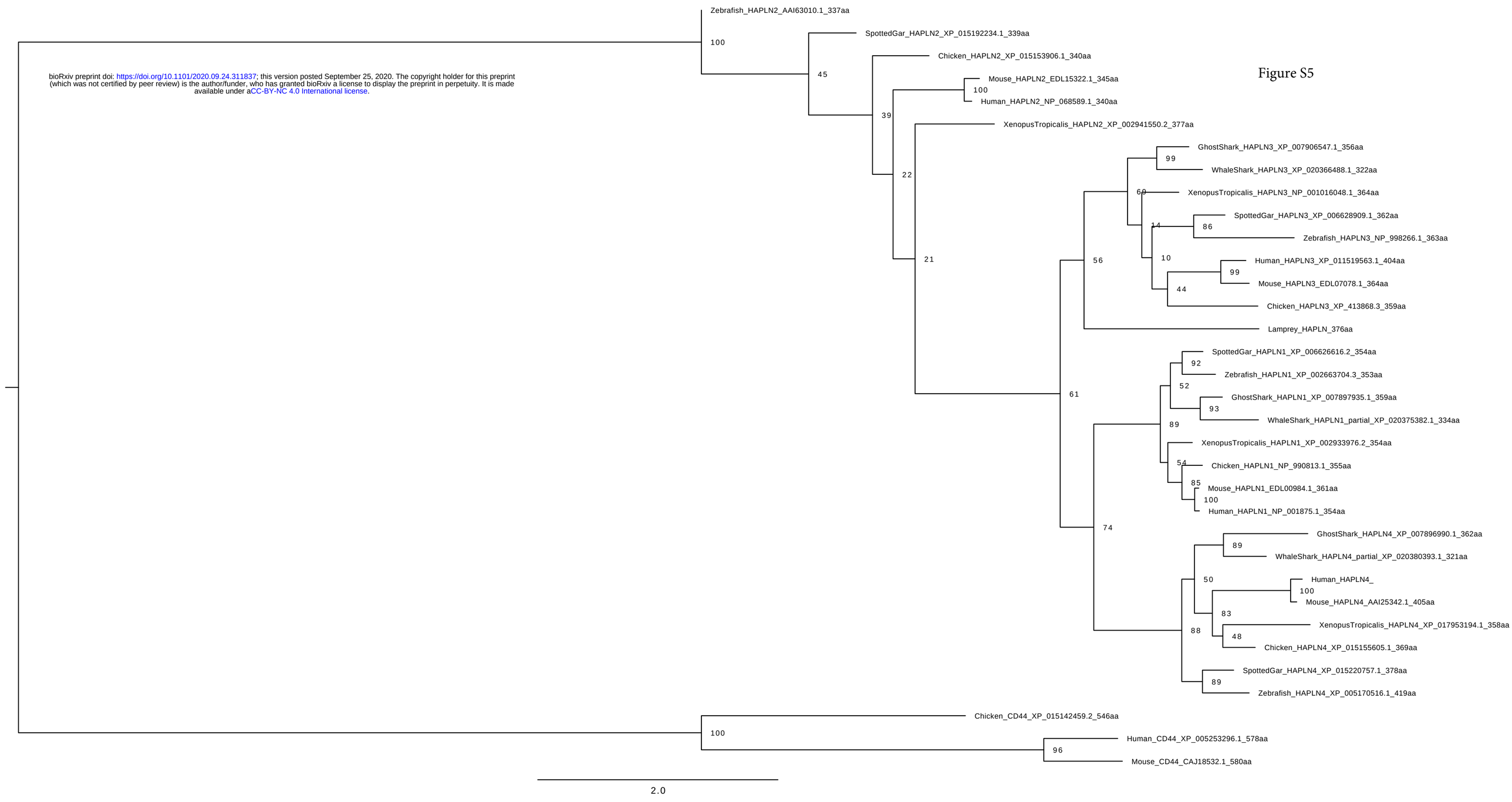

Figure S6

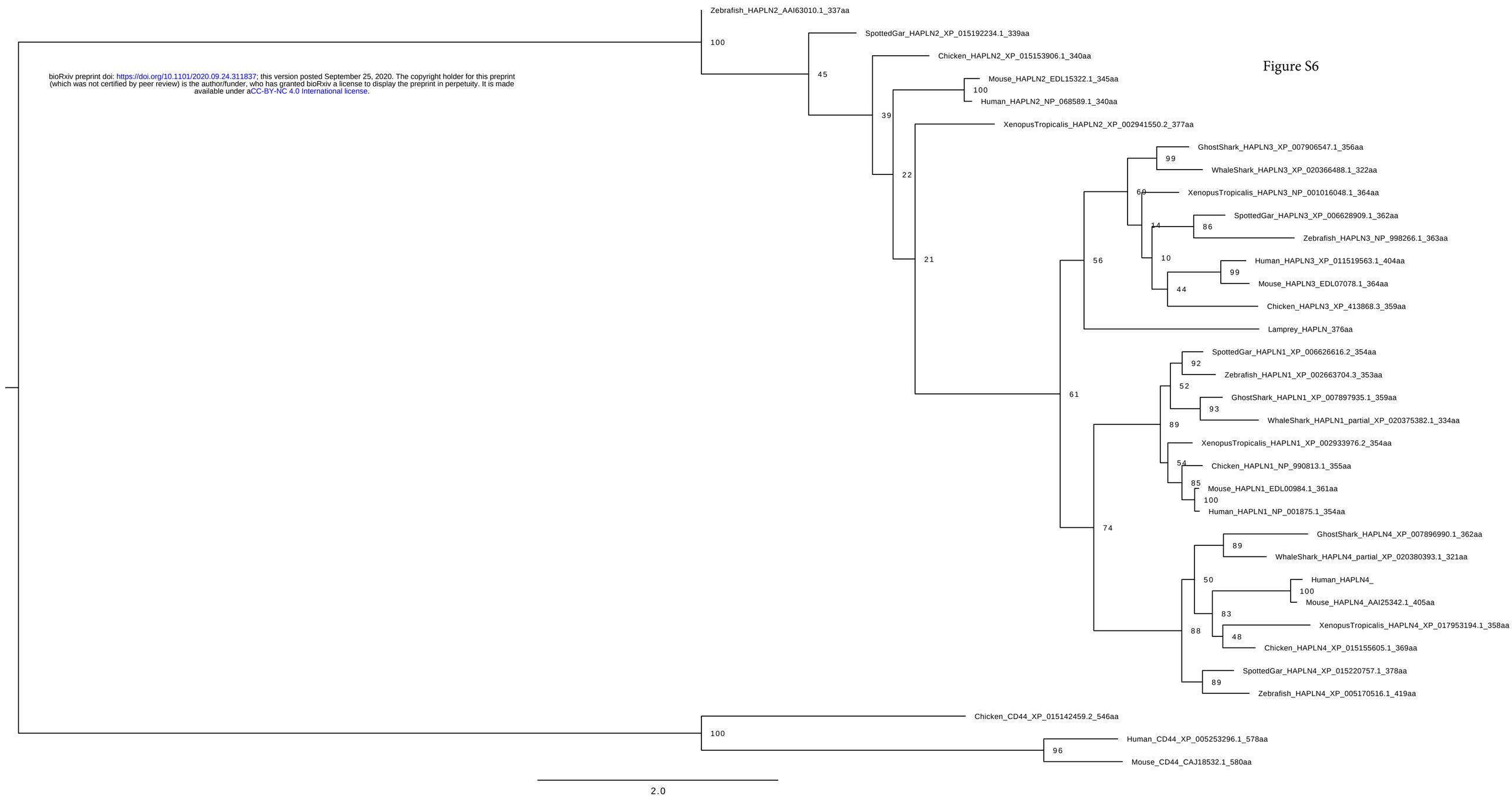

Figure S7

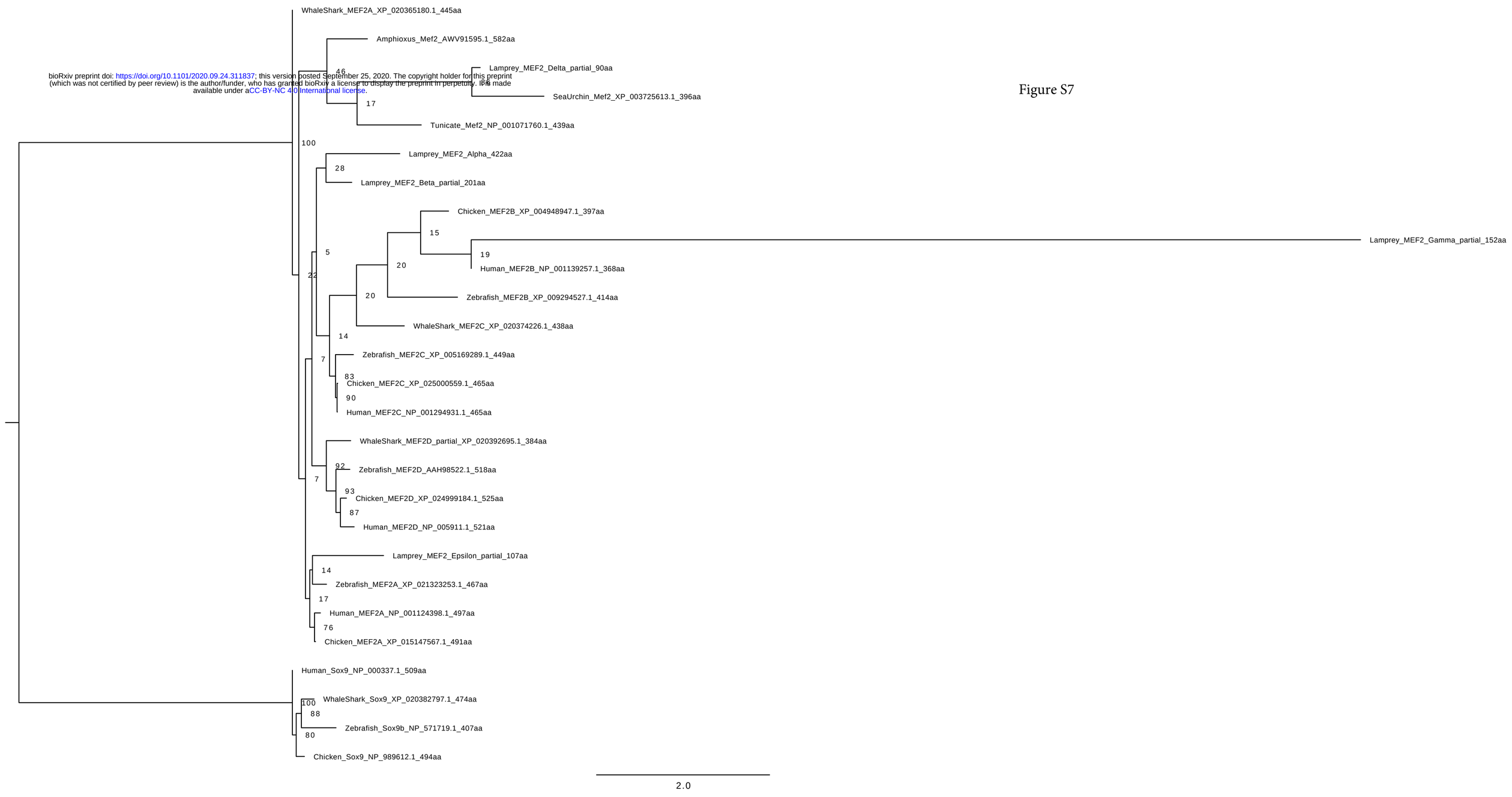

Figure S8

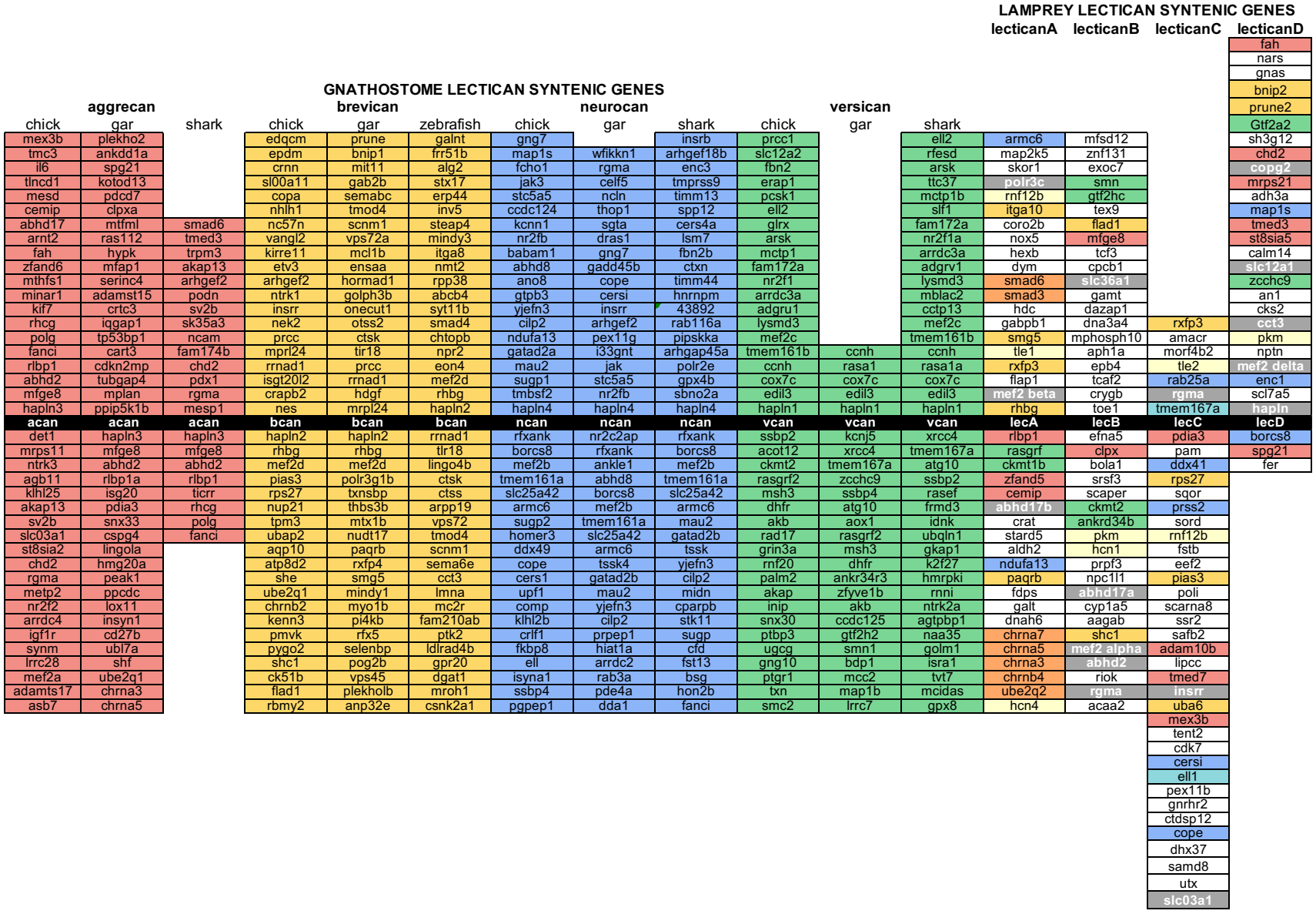
GNATHOSTOME LECTICAN SYNTENIC GENES
aggrecan
brevican
neurocan
versican
chick gar shark chick gar zebrafish chick gar shark chick gar shark
mex3b plekho2 edqcm prune galnt gng7 insrb prcc1 ell2
tmc3 ankdd1a epdm bnip1 frr51b map1s wfikkn1 arhgef18b slc12a2 rfesd
il6 spg21 crnn mit11 alg2 fcho1 rgma enc3 fbn2 arsk
tlncd1 kotod13 sl00a11 gab2b stx17 jak3 celf5 tmprss9 erap1 ttc37
mesd pdcd7 copa semabc erp44 stc5a5 ncln timm13 pcsk1 mctp1b
cemip clpxa nhlh1 tmod4 inv5 ccdc124 thop1 spp12 ell2 slf1
abhd17 mtfml smad6 nc57n scnm1 steap4 kcnn1 sgta cers4a glrx fam172a
arnt2 ras112 tmed3 vangl2 vps72a mindy3 nr2fb dras1 lsm7 arsk nr2f1a
fah hypk trpm3 kirre11 mcl1b itga8 babam1 gng7 fbn2b mctp1 arrdc3a
zfand6 mfap1 akap13 etv3 ensaa nmt2 abhd8 gadd45b ctxn fam172a adgrv1
mthfs1 serinc4 arhgef2 arhgef2 hormad1 rpp38 ano8 cope timm44 nr2f1 lysmd3
minar1 adamst15 podn ntrk1 golph3b abcb4 gtpb3 cersi hnrnpm arrdc3a mblac2
kif7 crtc3 sv2b insrr onecut1 syt11b yjefn3 insrr 43892 adgru1 cctp13
rhcg iqgap1 sk35a3 nek2 otss2 smad4 cilp2 arhgef2 rab116a lysmd3 mef2c
polg tp53bp1 ncam prcc ctsk chtopb ndufa13 pex11g pipskka mef2c tmem161b
fanci cart3 fam174b mprl24 tir18 npr2 gatad2a i33gnt arhgap45a tmem161b ccnh ccnh
rlbp1 cdkn2mp chd2 rrnad1 prcc eon4 mau2 jak polr2e ccnh rasa1 rasa1a
abhd2 tubgap4 pdx1 isgt20l2 rrnad1 mef2d sugp1 stc5a5 gpx4b cox7c cox7c cox7c
mfge8 mplan rgma crapb2 hdgf rhbg tmbsf2 nr2fb sbno2a edil3 edil3 edil3
hapln3 ppip5k1b mesp1 nes mrpl24 hapln2 hapln4 hapln4 hapln4 hapln1 hapln1 hapln1
acan acan acan bcan bcan bcan ncan ncan ncan vcan vcan vcan
det1 hapln3 hapln3 hapln2 hapln2 rrnad1 rfxank nr2c2ap rfxank ssbp2 kcnj5 xrcc4
mrps11 mfge8 mfge8 rhbg rhbg tlr18 borcs8 rfxank borcs8 acot12 xrcc4 tmem167a
ntrk3 abhd2 abhd2 mef2d mef2d lingo4b mef2b ankle1 mef2b ckmt2 tmem167a atg10
agb11 rlbp1a rlbp1 pias3 polr3g1b ctsk tmem161a abhd8 tmem161a rasgrf2 zcchc9 ssbp2
klhl25 isg20 ticrr rps27 txnsbp ctss slc25a42 borcs8 slc25a42 msh3 ssbp4 rasef
akap13 pdia3 rhcg nup21 thbs3b arpp19 armc6 mef2b armc6 dhfr atg10 frmd3
sv2b snx33 polg tpm3 mtx1b vps72 sugp2 tmem161a mau2 akb aox1 idnk
slc03a1 cspg4 fanci ubap2 nudt17 tmod4 homer3 slc25a42 gatad2b rad17 rasgrf2 ubqln1
st8sia2 lingola aqp10 paqrb scnm1 ddx49 armc6 tssk grin3a msh3 gkap1
chd2 hmg20a atp8d2 rxfp4 sema6e cope tssk4 yjefn3 rnf20 dhfr k2f27
rgma peak1 she smg5 cct3 cers1 gatad2b cilp2 palm2 ankr34r3 hmrpki
metp2 ppcdc ube2q1 mindy1 lmna upf1 mau2 midn akap zfyve1b rnni
nr2f2 lox11 chrnb2 myo1b mc2r comp yjefn3 cparpb inip akb ntrk2a
arrdc4 insyn1 kenn3 pi4kb fam210ab klhl2b cilp2 stk11 snx30 ccdc125 agtpbp1
igf1r cd27b pmvk rfx5 ptk2 crlf1 prpep1 sugp ptbp3 gtf2h2 naa35
synm ubl7a pygo2 selenbp ldlrad4b fkbp8 hiat1a cfd ugcg smn1 golm1
lrrc28 shf shc1 pog2b gpr20 ell arrdc2 fst13 gng10 bdp1 isra1
mef2a ube2q1 ck51b vps45 dgat1 isyna1 rab3a bsg ptgr1 mcc2 tvt7
adamts17 chrna3 flad1 plekholb mroh1 ssbp4 pde4a hon2b txn map1b mcidas
asb7 chrna5 rbmy2 anp32e csnk2a1 pgpep1 dda1 fanci smc2 lrrc7 gpx8
LAMPREY LECTICAN SYNTENIC GENES
lecticanA lecticanB lecticanC lecticanD
armc6 mfsd12 fah
map2k5 znf131 nars
skor1 exoc7 gnas
polr3c smn bnip2
rnf12b gtf2hc prune2
itga10 tex9 Gtf2a2
coro2b flad1 sh3g12
nox5 mfge8 chd2
hexb tcf3 copg2
dym cpcb1 mrps21
smad6 slc36a1 adh3a
smad3 gamt map1s
hdc dazap1 tmed3
gabpb1 dna3a4 rxfp3 st8sia5
smg5 mphosph10 amacr calm14
tle1 aph1a morf4b2 slc12a1
rxfp3 epb4 tle2 zcchc9
flap1 tcaf2 rab25a an1
mef2 beta crygb rgma cks2
rhbg toe1 tmem167a cct3
lecA lecB lecC lecD
rlbp1 efna5 pdia3 borcs8
rasgrf clpx pam spg21
ckmt1b bola1 ddx41 fer
zfand5 srsf3 rps27
cemip scaper sqor
abhd17b ckmt2 prss2
crat ankrd34b sord
stard5 pkm rnf12b
aldh2 hcn1 fstb
ndufa13 prpf3 eef2
paqrb npc1l1 pias3
fdps abhd17a poli
galt cyp1a5 scarna8
dnah6 aagab ssr2
chrna7 shc1 safb2
chrna5 mef2 alpha adam10b
chrna3 abhd2 lipcc
chrnb4 riok tmed7
ube2q2 rgma insrr
hcn4 acaa2 uba6
mex3b
tent2
cdk7
cersi
ell1
pex11b
gnrhr2
ctdsp12
cope
dhx37
samd8
utx
slc03a1

Table S1. NCBI accession numbers used for the phylogenetic analysis in Figure S1

Sequence Name	**Accession Number**
Lamprey_HAPLN	MT125613
Mouse_HAPLN1	EDL00984.1
ClawedFrog_HAPLN1	XP_002933976.2
GhostShark_HAPLN1	XP_007897935.1
WhaleShark_HAPLN1	XP_020375382.1
Human_HAPLN1	NP_001875.1
Chicken_HAPLN1	NP_990813.1
SpottedGar_HAPLN1	XP_006626616.2
Zebrafish_HAPLN1	XP_002663704.3
Mouse_HAPLN2	EDL15322.1
ClawedFrog_HAPLN2	XP_002941550.2
Human_HAPLN2	NP_068589.1
Chicken_HAPLN2	XP_015153906.1
SpottedGar_HAPLN2	XP_015192234.1
Zebrafish_HAPLN2	AAI63010.1
Mouse_HAPLN3	EDL07078.1
ClawedFrog_HAPLN3	NP_001016048.1
GhostShark_HAPLN3	XP_007906547.1
WhaleShark_HAPLN3	XP_020366488.1
Human_HAPLN3	XP_011519563.1
Chicken_HAPLN3	XP_413868.3
SpottedGar_HAPLN3	XP_006628909.1
Zebrafish_HAPLN3	NP_998266.1
Mouse_HAPL4	AAI25342.1
ClawedFrog_HAPLN4	XP_017953194.1
GhostShark_HAPLN4	XP_007896990.1

WhaleShark_HAPLN4	XP_020380393.1
Human_HAPLN4	NP_075378.1
Chicken_HAPLN4	XP_015155605.1
SpottedGar_HAPLN4	XP_015220757.1
Zebrafish_HAPLN4	XP_005170516.1
Mouse_CD44	CAJ18532.1
Human_CD44	XP_005253296.1
Chicken_CD44	XP_015142459.2

Table S2. NCBI accession numbers used for the phylogenetic analysis in Figure S2

Lamprey_LecA	MT125609
Lamprey_LecB	MT125610
Lamprey_LecC	MT125611
Lamprey_LecD	MT125612
Lamprey_HAPLN	MT125613
EptatretusBurgeri_Lec1	MT559761
EptatretusBurgeri_Lec2	MT559762
EptatretusBurgeri_Lec3	MT582507
EptatretusBurgeri_HAPLN	MT559763
Amphioxus_HAPLN3-like_partial	MT582506
Human_ACAN	EAX02019.1
Chicken_ACAN	XP_015147465.1
GhostShark_ACAN	XP_007906559.1
Human_VCAN	NP_004376.2
Chicken_VCAN	XP_015136072.1
GhostShark_VCAN	XP_007898000.1
GhostShark_BCAN	AGN91175.1

Chicken_BCAN	XP_015153902.1
Human_BCAN	XP_016857536.1
Human_NCAN	AAC80576.1
Chicken_NCAN	NP_990071.1
GhostShark_NCAN	XP_007896991.1
Mouse_HAPLN1	EDL00984.1
ClawedFrog_HAPLN1	XP_002933976.2
GhostShark_HAPLN1	XP_007897935.1
WhaleShark_HAPLN1	XP_020375382.1
Human_HAPLN1	NP_001875.1
Chicken_HAPLN1	NP_990813.1
SpottedGar_HAPLN1	XP_006626616.2
Zebrafish_HAPLN1	XP_002663704.3
Mouse_HAPLN2	EDL15322.1
ClawedFrog_HAPLN2	XP_002941550.2
Human_HAPLN2	NP_068589.1
Chicken_HAPLN2	XP_015153906.1
SpottedGar_HAPLN2	XP_015192234.1
Zebrafish_HAPLN2	AAI63010.1
Mouse_HAPLN3	EDL07078.1
ClawedFrog_HAPLN3	NP_001016048.1
GhostShark_HAPLN3	XP_007906547.1
WhaleShark_HAPLN3	XP_020366488.1
Human_HAPLN3	XP_011519563.1
Chicken_HAPLN3	XP_413868.3
SpottedGar_HAPLN3	XP_006628909.1
Zebrafish_HAPLN3	NP_998266.1
Mouse_HAPL4	AAI25342.1

ClawedFrog_HAPLN4	XP_017953194.1
GhostShark_HAPLN4	XP_007896990.1
WhaleShark_HAPLN4	XP_020380393.1
Human_HAPLN4	NP_075378.1
Chicken_HAPLN4	XP_015155605.1
SpottedGar_HAPLN4	XP_015220757.1
Zebrafish_HAPLN4	XP_005170516.1
Mouse_CD44	CAJ18532.1
Human_CD44	XP_005253296.1
Chicken_CD44	XP_015142459.2
Tunicate_Lactadherin	XP_009859662.1
Amphioxus_HAPLN2-like_partial	XP_019631180.1
Amphioxus_HAPLN3-like_partial	XP_019641525.1

Table S3. NCBI accession numbers used for the phylogenetic analysis in Figures S3 and S4

Lamprey_LecA	MT125609
Lamprey_LecB	MT125610
Lamprey_LecC	MT125611
Lamprey_LecD	MT125612
Human_ACAN	XP_011519615.1
Zebrafish_ACAN	XP_021333626.1
ClawedFrog_ACAN	XP_031755090.1
Human_BCAN	AAH09117.1
Zebrafish_BCAN	NP_001077282.1
ClawedFrog_BCAN	XP_004917415.2
Human_NCAN	NP_004377.2
Zebrafish_NCAN	XP_017208935.1
ClawedFrog_NCAN	XP_012810121.1

Human_VCAN	NP_004376.2
Zebrafish_VCAN	NP_999853.1
ClawedFrog_VCAN	XP_002935750.2
Human_HAPLN1	AAH57808.1
Zebrafish_HAPLN1	XP_002663704.3
ClawedFrog_HAPLN1	XP_002933976.2

Table S4. NCBI accession numbers used for the phylogenetic analysis in Figure S5

Sequence Name	**Accession Number**
Lamprey_LecA	MT125609
Lamprey_LecB	MT125610
Lamprey_LecC	MT125611
Lamprey_LecD	MT125612
Human_ACAN	EAX02019.1
Chicken_ACAN	XP_015147465.1
Zebrafish_ACAN	XP_021329528.1
GhostShark_ACAN	XP_007906559.1
Human_VCAN	NP_004376.2
Chicken_VCAN	XP_015136072.1
Zebrafish_Dermacan	NP_999853.1
GhostShark_VCAN	XP_007898000.1
Zebrafish_VCAN	NP_001313486.1
GhostShark_BCAN	AGN91175.1
Chicken_BCAN	XP_015153902.1
Human_BCAN	XP_016857536.1
Zebrafish_BCAN	NP_001077282.1
Human_NCAN	AAC80576.1
Chicken_NCAN	NP_990071.1

Zebrafish_NCAN	XP_017208935.1
GhostShark_NCAN	XP_007896991.1
Mouse_HAPLN1	EDL00984.1
Human_HAPLN1	NP_001875.1
Chicken_HAPLN1	NP_990813.1

Table S5. NCBI accession numbers used for the phylogenetic analysis in Figure S6

Lamprey_LecA	MT125609
Lamprey_LecB	MT125610
Lamprey_LecC	MT125611
Lamprey_LecD	MT125612
EptatretusBurgeri_Lec1	MT559761
EptatretusBurgeri_Lec2	MT559762
Human_ACAN	EAX02019.1
Chicken_ACAN	XP_015147465.1
Zebrafish_ACAN	XP_021329528.1
GhostShark_ACAN	XP_007906559.1
Mouse_ACAN	AAC37670.1
ClawedFrog_ACAN	XP_018106934.1
WhaleShark_ACAN	XP_020366487.1
SpottedGar_ACAN	XP_015198823.1
Sturgeon_ACAN	GGZX01639449.1
Human_VCAN	NP_004376.2
Chicken_VCAN	XP_015136072.1
GhostShark_VCAN	XP_007898000.1
Zebrafish_VCAN	NP_999853.1
Mouse_VCAN	XP_011242772.1
SpottedGar_VCAN	XP_015216137.1

ClawedFrog_VCAN	XP_018081624.1
WhaleShark_VCAN	XP_020375390.1
Sturgeon_VCAN	GGWJ01016472.1
GhostShark_BCAN	AGN91175.1
Chicken_BCAN	XP_015153902.1
Human_BCAN	XP_016857536.1
Zebrafish_BCAN	NP_001077282.1
Mouse_BCAN	CAA60575.1
SpottedGar_BCAN	XP_015192104.1
ClawedFrog_BCAN	XP_018088981.1
Human_NCAN	AAC80576.1
Chicken_NCAN	NP_990071.1
Zebrafish_NCAN	XP_017208935.1
GhostShark_NCAN	XP_007896991.1
Mouse_NCAN	CAA59216.1
ClawedFrog_NCAN	XP_018095360.1
SpottedGar_NCAN	XP_015221289.1
WhaleShark_NCAN	XP_020377172.1
Mouse_HAPLN1	EDL00984.1
Human_HAPLN1	NP_001875.1
Chicken_HAPLN1	NP_990813.1

Table S6. NCBI accession numbers used for the phylogenetic analysis in Figure S7

Lamprey_Mef2Alpha	MT559756
Lamprey_Mef2Beta	MT559757
Lamprey_Mef2Gamma	MT559758
Lamprey_Mef2Delta	MT559759

Lamprey_Mef2Epsilon	MT559760
Human_Mef2A	NP_001124398.1
Chicken_Mef2A	XP_015147567.1
Zebrafish_Mef2A	XP_021323253.1
WhaleShark_Mef2A	XP_020365180.1
Human_Mef2B	NP_001139257.1
Chicken_Mef2B	XP_004948947.1
Zebrafish_Mef2B	XP_009294527.1
Human_Mef2C	NP_001294931.1
Chicken_Mef2C	XP_025000559.1
Zebrafish_Mef2C	XP_005169289.1
WhaleShark_Mef2C	XP_020374226.1
Human_Mef2D	NP_005911.1
Chicken_Mef2D	XP_024999184.1
Zebrafish_Mef2D	AAH98522.1
WhaleShark_Mef2D	XP_020392695.1
Tunicate_Mef2	NP_001071760.1
Amphioxus_Mef2	AWV91595.1
SeaUrchin_Mef2	XP_003725613.1
Human_Sox9	NP_000337.1
Chicken_Sox9	NP_989612.1
Zebrafish_Sox9	NP_571719.1
WhaleShark_Sox9	XP_020382797.1